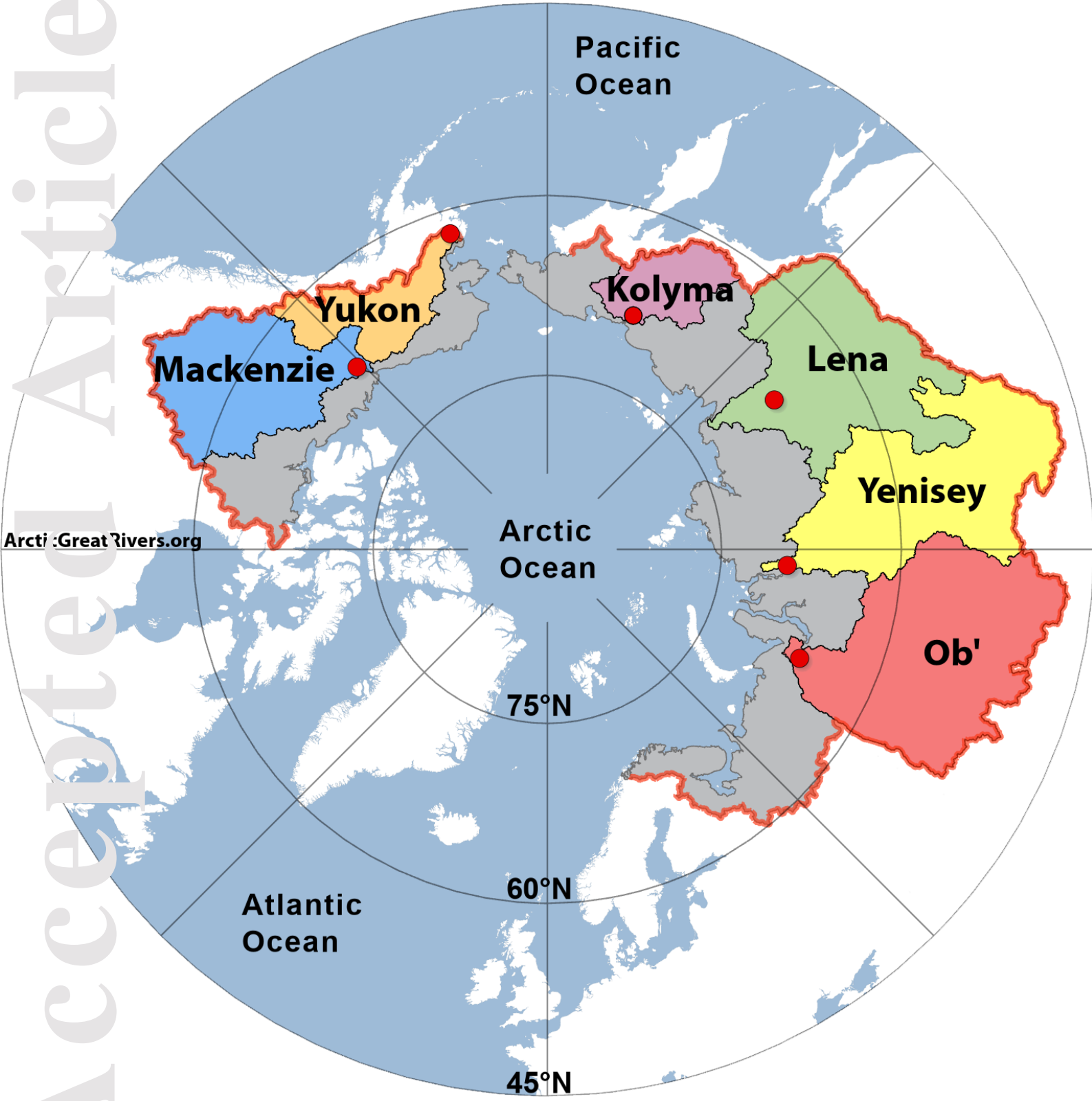

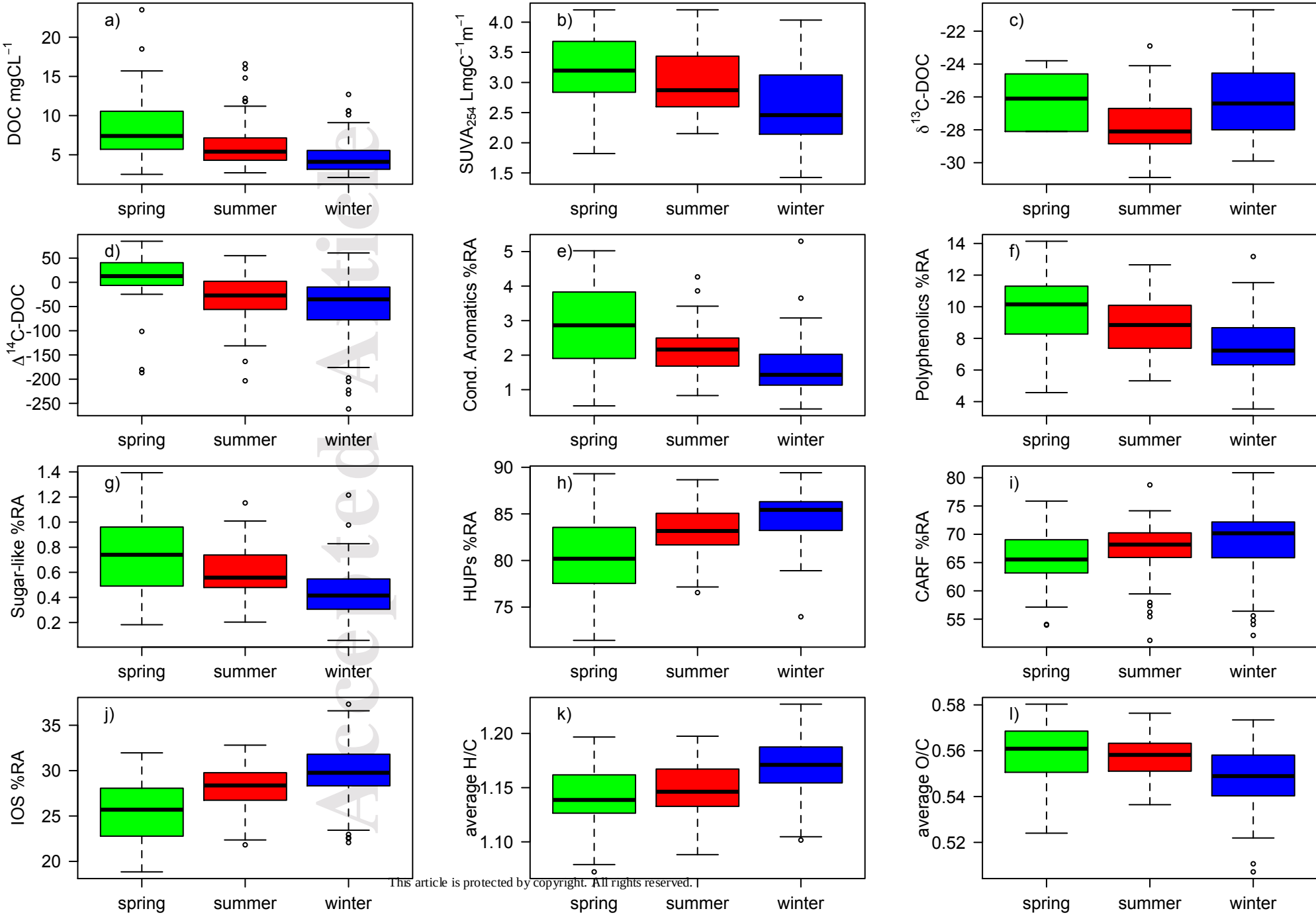

a)

CHONS
CHOS
CHON
Sugar-like
Aliphatics
Polyphenolics
Condensed Aromatics
$SUVA_{254}$
DOC
δ^{13}C-DOC
Peptide-like
Δ^{14}C-DOC
HUPs
CHO

PC2 (17.36%)
PC1 (39.82%)

b)

Ob’
Yenisey
Lena
Kolyma
Yukon
Mackenzie

Spring
Summer
Winter

PC2 (17.36%)
PC1 (39.82%)

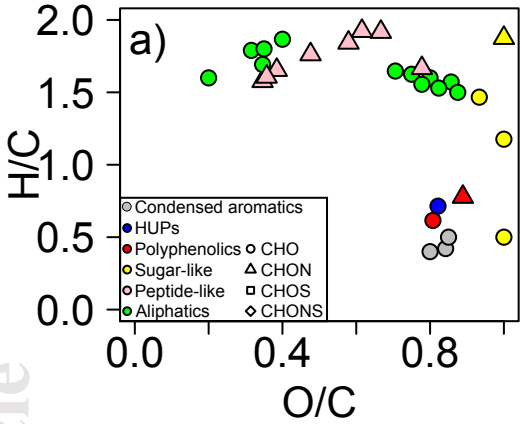

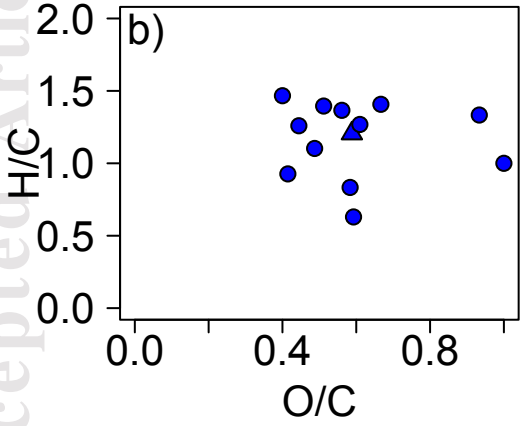

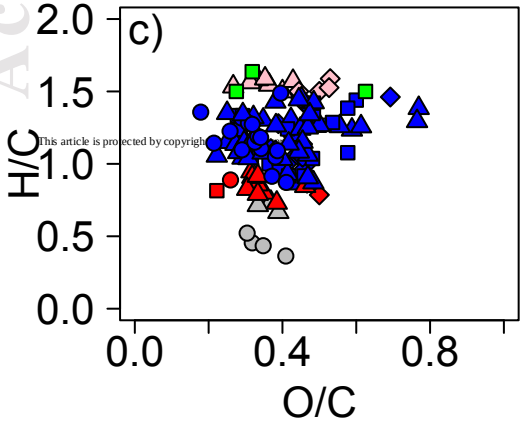

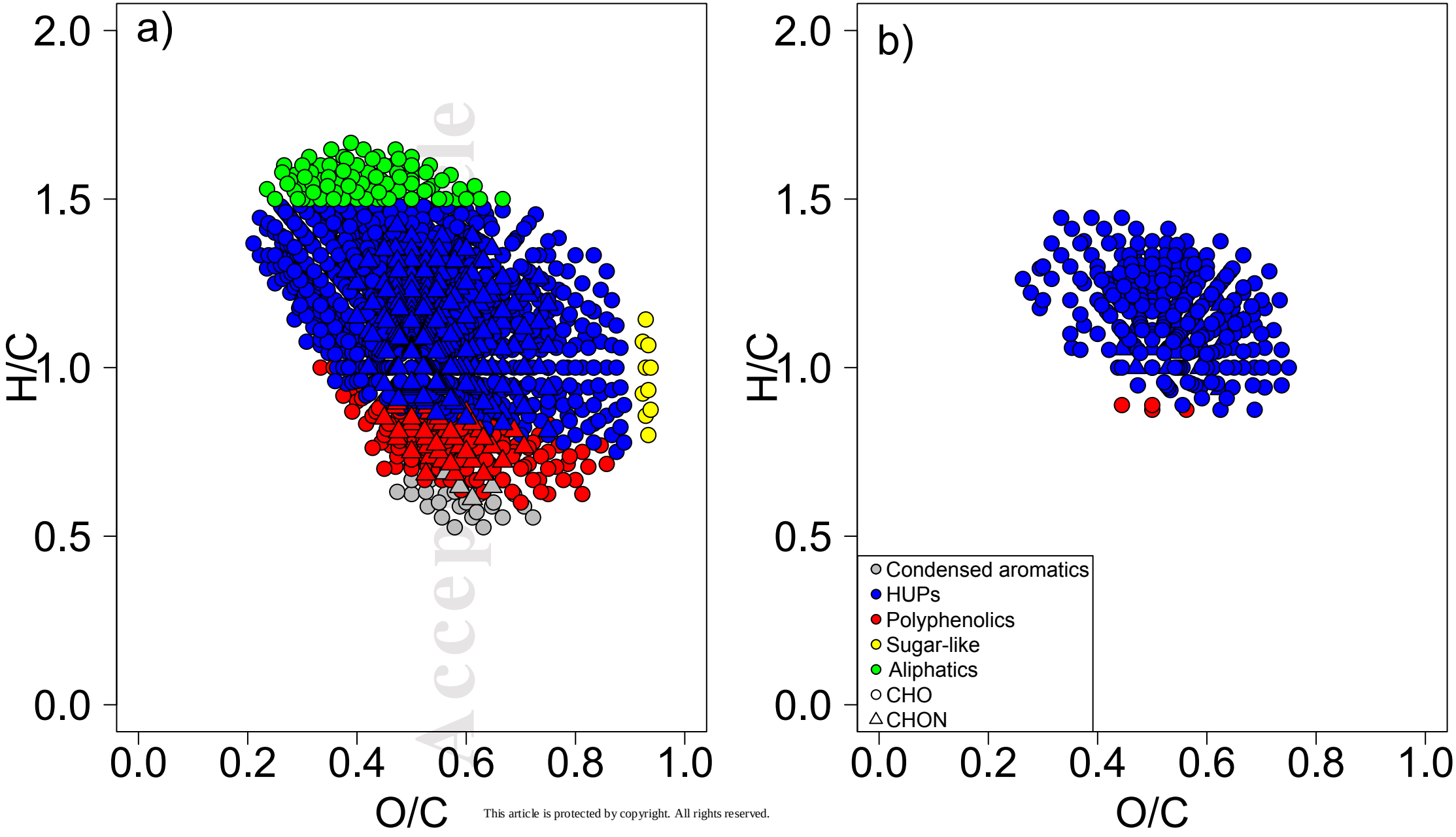

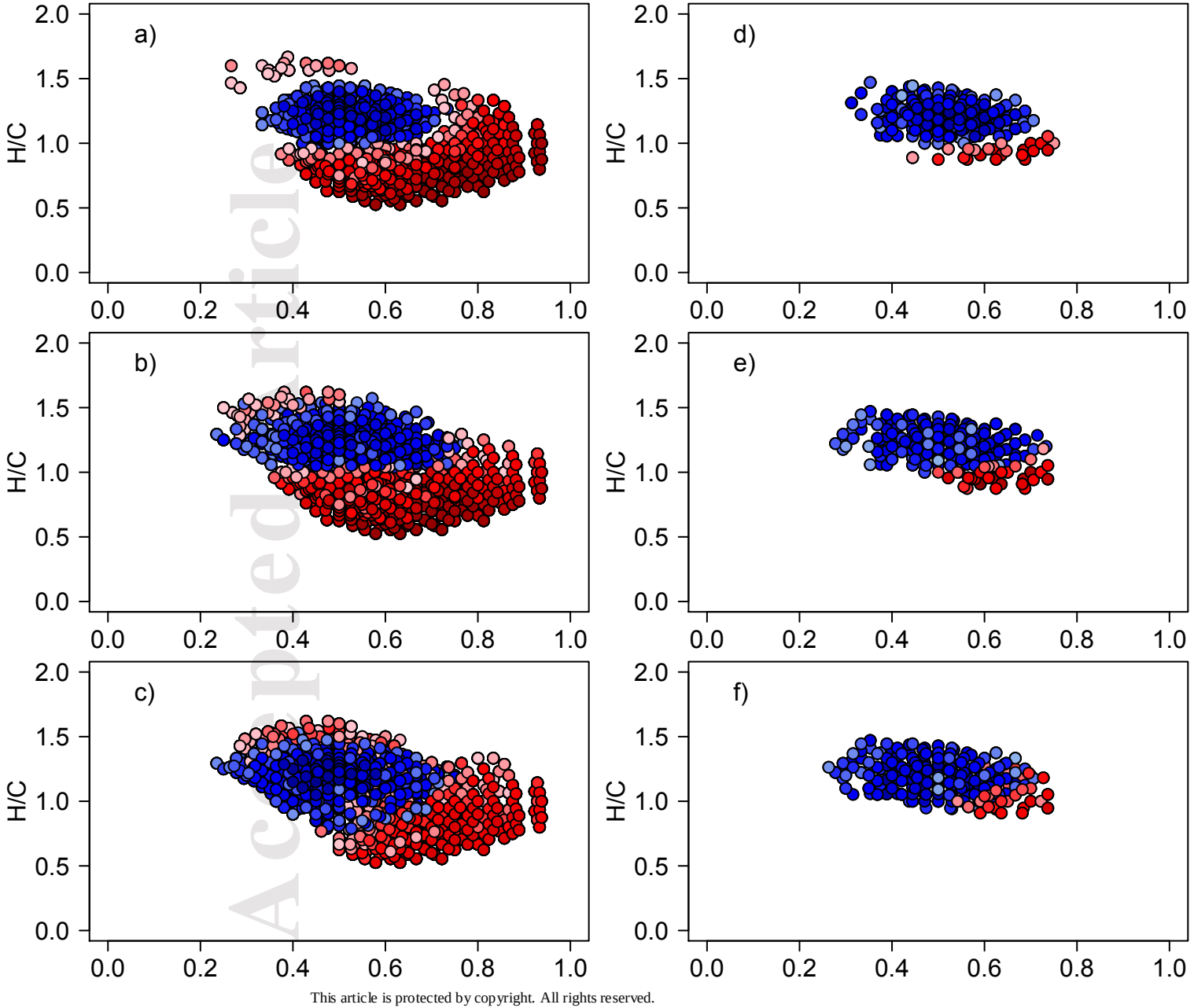

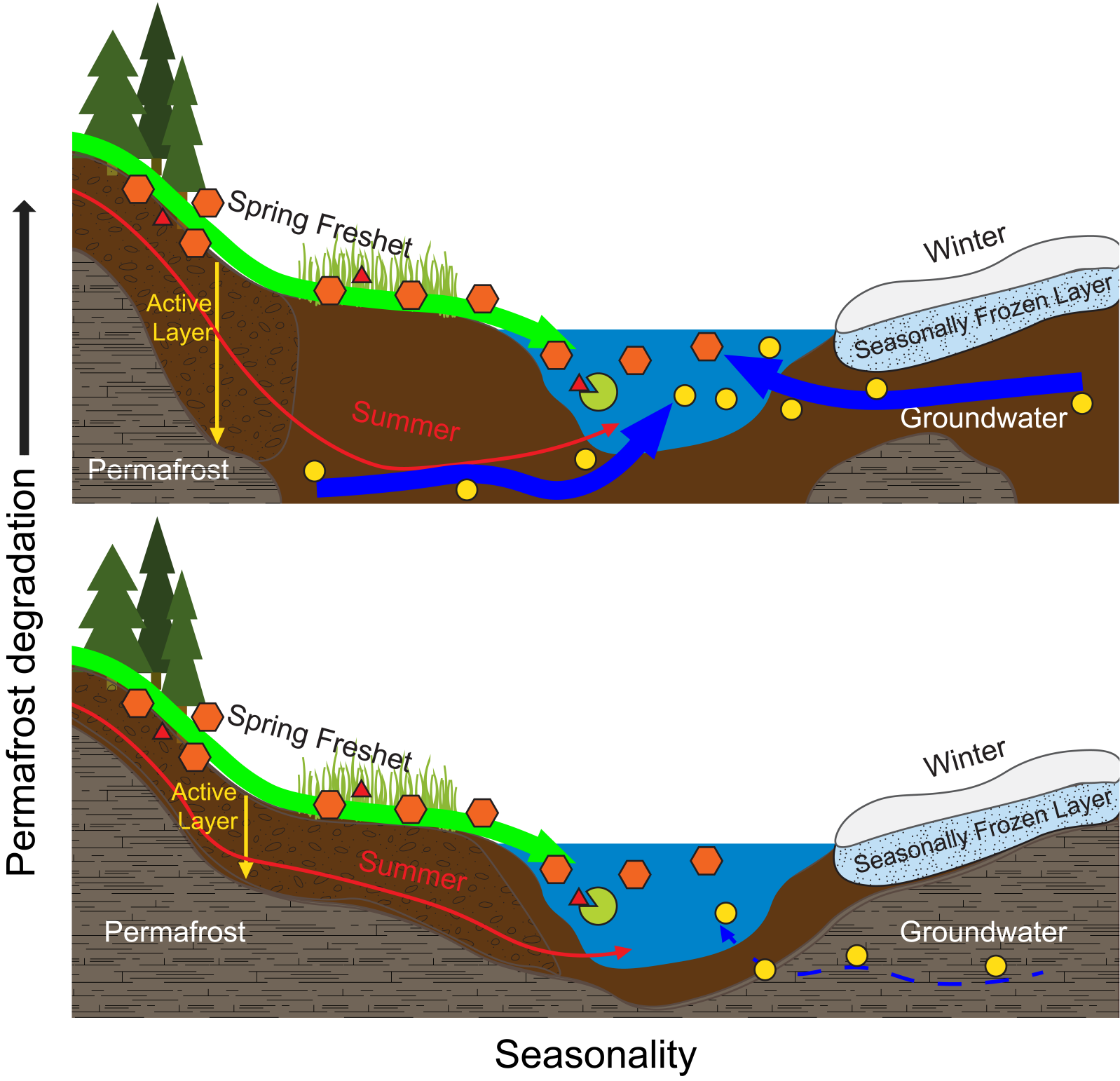
Permafrost degradation
Spring Freshet
Active Layer
Summer
Permafrost
Winter
Seasonally Frozen Layer
Groundwater
Spring Freshet
Active Layer
Summer
Permafrost
Winter
Seasonally Frozen Layer
Groundwater
Seasonality

Pan-Arctic riverine dissolved organic matter: Synchronous molecular stability, shifting sources and subsidies

M. I. Behnke[1*], J. W. McClelland[2], S. E. Tank[3], A. M. Kellerman[1], R. M. Holmes[4], N. Haghipour[5,6], T. I. Eglinton[5], P. A. Raymond[7], A. Suslova[4], A. V. Zhulidov[8], T. Gurtovaya[8], N. Zimov[9], S. Zimov[9], E. A. Mutter[10], E. Amos[11], R. G. M. Spencer[1]

[1]National High Magnetic Field Laboratory Geochemistry Group and Department of Earth, Ocean, and Atmospheric Science, Florida State University, Tallahassee FL (United States)

[2]University of Texas Marine Science Institute Port Aransas TX (United States)

[3]University of Alberta Biological Sciences Edmonton AB (Canada)

[4]Woodwell Climate Research Center Falmouth MA (United States)

[5]Department of Earth Sciences, Geological Institute, ETH Zurich (Switzerland)

[6]Laboratory for Ion Beam Physics, ETH Zurich (Switzerland)

[7]School of Forestry & Environmental Studies, Yale University, New Haven CT (United States)

[8]South Russia Centre for Preparation and Implementation of International Projects, Rostov-on-Don (Russia)

[9]Northeast Science Station, Far Eastern Branch of Russian Academy of Science, Chersky (Russia)

[10]Yukon River Inter-Tribal Watershed Council, Anchorage, Alaska (United States)

[11]Western Arctic Research Centre, Inuvik, Northwest Territories (Canada)

*Corresponding Author: E-mail: mibehnke@fsu.edu

Co-author E-mails: J.W.M.: jimm@utexas.edu; S.E.T.: suzanne.tank@ualberta.ca; A.M.K.: akellerman@fsu.edu; R.M.H.: rmholmes@woodwellclimate.org; N.H.: negar.haghipour@erdw.ethz.ch; T.I.E.: timothy.eglinton@erdw.ethz.ch; P.A.R.: peter.raymond@yale.edu; A.S.: asuslova@woodwellclimate.org; A.V.Z.: zhulidov@cppis.ru; T.G.: tanya@cppis.ru; N.Z.: nzimov@mail.ru; S.Z.: sazimov@cher.sakha.ru; E.A.M.: emutter@yritwc.org; E.A.: edwin.amos@auroracollege.nt.ca; R.G.M.S.: rgspencer@magnet.fsu.edu

Key Points

1) Synchrony: Ultrahigh-resolution mass spectrometry shows seasonality controls dissolved organic matter composition in six large Arctic rivers

2) Stability: A core Arctic riverine fingerprint was found in all rivers and months for six years and may add stable carbon to the global ocean

3) Shifting sources: Permafrost thaw may increase old, stable carbon load via increasing groundwater inputs and microbial processing time

Abstract

Climate change is dramatically altering Arctic ecosystems, leading to shifts in the sources, composition, and eventual fate of riverine dissolved organic matter (DOM) in the Arctic Ocean. Here we examine a six-year DOM compositional record from the six major Arctic rivers using Fourier-transform ion cyclotron resonance mass spectrometry paired with dissolved organic carbon isotope data ($\Delta^{14}C$, $\delta^{13}C$) to investigate how seasonality and permafrost influence DOM, and how DOM export may change with warming. Across the pan-Arctic, DOM molecular composition demonstrates synchrony and stability. Spring freshet brings recently leached terrestrial DOM with a latent high-energy and potentially bioavailable subsidy, reconciling the historical paradox between freshet DOM's terrestrial bulk signatures and high biolability. Winter features undiluted baseflow DOM sourced from old, microbially degraded groundwater DOM. A stable core Arctic riverine fingerprint (CARF) is present in all samples and may contribute to the potential carbon sink of persistent, aged DOM in the global ocean. Future warming may lead to shifting sources of DOM and export through: 1) flattening Arctic hydrographs and earlier melt modifying the timing and role of the spring high-energy subsidy; 2) increasing groundwater discharge resulting in a greater fraction of DOM export to the ocean occurring as stable and aged molecules; and 3) increasing contribution of nitrogen/sulfur-containing DOM from microbial degradation caused by increased connectivity between groundwater and surface waters due to permafrost thaw. Our findings suggest the ubiquitous CARF (which may contribute to oceanic carbon sequestration) underlies predictable variations in riverine DOM composition caused by seasonality and permafrost extent.

Plain Language Summary

Climate change is causing the Arctic to warm, leading to the thaw of permafrost (permanently frozen ground) and shifting the distribution of plants, which in turn impact the quantity and quality of dissolved organic matter (DOM) in rivers. The fate of the carbon found in river DOM depends on its source as this determines its composition – a smorgasbord of organic substrates with some destined to be rapidly turned into greenhouse gases through respiration, while others may be exported to and sequestered in the ocean for millennia. Understanding the sources and composition of DOM presently in Arctic rivers will help predict future changes in the global carbon cycle. In this study we examine six years of data on the composition of DOM found in the six largest Arctic rivers (sampled by the Arctic Great Rivers Observatory). Overall, our work suggests that DOM in large Arctic rivers contains a universal core Arctic riverine fingerprint (which may contribute to long-term ocean carbon sequestration), and that there are predictable, pan-Arctic seasonal changes in DOM composition. Finally, we explore how future warming may shift DOM sources in Arctic rivers, particularly due to increasing groundwater inputs to rivers caused by thawing permafrost in the region.

Keywords:

Dissolved organic matter, rivers, Arctic, permafrost, FT-ICR MS, radiocarbon

Index terms:

0414 Biogeochemical cycles, processes, and modeling; 0428 Carbon cycling; 0454 Isotopic composition and chemistry; 0475 Permafrost, cryosphere, and high-latitude processes; 0744 Rivers

1. Introduction

Climate change–induced warming is greatest in the Arctic, invoking globally significant shifts in atmospheric circulation, carbon cycling, and permafrost stability and extent (Serreze & Barry, 2011). The northern permafrost region stores ~1500 Pg of soil organic carbon (Schuur et al., 2015). Carbon in perennially frozen ground (permafrost) is vulnerable to warming-induced thaw, emission as greenhouse gases, erosion from abrupt thaw processes and riverine transport as particulate organic matter, and lateral aqueous transport as dissolved organic matter (DOM) (Schuur et al., 2015; Turetsky et al., 2020). Permafrost controls hydrology, and thaw can alter groundwater flow and river discharge (Walvoord & Kurylyk, 2016). Arctic river discharge and direct groundwater inputs are so significant in the small Arctic Ocean Basin that the Arctic Ocean itself has been described as a giant estuary (Connolly et al., 2020; Holmes et al., 2012; Kaiser et al., 2017; McClelland et al., 2012). Changes in freshwater inputs could impact ocean stratification and circulation (Arnell, 2005). When combined with potential changes in exported riverine DOM composition and bioavailability, such changes in ocean structure could alter heterotrophic metabolism, nutrient regeneration, and subsequent primary production (Holmes et al., 2008; Mann et al., 2016). River runoff contributes to Arctic Ocean carbon dioxide (CO_2) drawdown potential not only through total alkalinity export but also through respiration of exported DOM (Drake, Tank, et al., 2018; Tank et al., 2012; Tremblay et al., 2015). If Arctic river DOM becomes more plentiful or bioavailable, this could alter the Arctic Ocean's carbon sink capacity (Tremblay et al., 2015). Understanding the controls of Arctic riverine DOM is therefore critical, as

warming landscapes may lead to DOM changes impacting pan-Arctic greenhouse gas production and sequestration.

Large Arctic rivers integrate all processes and features present in their watersheds, providing a holistic snapshot of the state of the Arctic landscape (Holmes et al., 2013). The fate and reactivity of riverine DOM (a complex mixture of degradation byproducts and recently created compounds) is linked to its composition (Kellerman et al., 2015; Smith, H. J. et al., 2018). In turn, composition depends on source and processing history (Kellerman et al., 2014; Stubbins et al., 2010). Measurements of stable isotope ratios and radiocarbon content have long been used to help identify DOM sources (Connolly et al., 2020; Fellman et al., 2014; Raymond & Bauer, 2001a). In addition to these classic bulk measurements, recent advances in Fourier-transform ion cyclotron resonance mass spectrometry (FT-ICR MS) now allow unparalleled insights into DOM composition by identifying thousands of individual formulae present in DOM to enable elucidation of trends in DOM composition across systems and through time (Antony et al., 2017; Johnston et al., 2018; Spencer et al., 2019). FT-ICR MS has been used to examine DOM sources in diverse aquatic systems, including rivers (e.g. Drake, Guillemette, et al., 2018; Spencer et al., 2019), groundwater (e.g. McDonough, Rutlidge, et al., 2020) and lakes (e.g. Johnston et al., 2019; Kellerman et al., 2015). Combined, carbon isotope and FT-ICR MS data offer a powerful tool to assess DOM sources and the processes controlling them (Behnke et al., 2020; McDonough, Rutlidge, et al., 2020; Stubbins et al., 2017).

Here, we assess seasonal controls of DOM composition in Arctic rivers using ultrahigh resolution mass spectrometry combined with traditional DOM measurements such as optical (e.g. specific UV-absorbance at 254 nm, which has been shown to be a

robust proxy for aromaticity; Weishaar et al., 2003) and isotopic ($\delta^{13}C$ and $\Delta^{14}C$) data. We examine seasonal and spatial variability in DOM molecular composition. Using molecular-level analysis, we attempt to explain the historical paradox between the bulk DOM signatures of Arctic spring freshet that appear terrestrial and aromatic yet exhibit high biolability. Further, we assess the prevalence of stable DOM in Arctic rivers by examining the dominant and persistent core Arctic riverine fingerprint (CARF), and we determine whether Arctic rivers could be a source of stable DOM such as the "island of stability" compositional region that persists in the global ocean (and that may serve as an oceanic carbon sink; Jiao et al., 2010; Lechtenfeld et al., 2014). We also explore how differences in DOM composition among rivers relate to differences in watershed permafrost extent. To achieve these goals, we examine six years (2012–2017) of FT-ICR MS data on DOM molecular formulae (to our knowledge, the longest time-series study employing FT-ICR MS yet conducted), dissolved organic carbon (DOC) concentrations, and DOC radiocarbon and stable carbon isotope ratio data for the six largest Arctic rivers (the Ob', Yenisey, Lena, Kolyma, Yukon, and Mackenzie; Arctic Great Rivers Observatory; www.arcticgreatrivers.org; Fig. 1). We use the knowledge we gain of the controls on DOM composition to begin assessing how climate change could modify Arctic riverine DOM composition and what impacts such changes could have on Arctic Ocean biogeochemistry, productivity, and carbon storage.

2. Methods

2.1 Study locations and sample collection

Samples from the six largest Arctic rivers were collected as part of the Arctic Great Rivers Observatory (Fig. 1). Each river was sampled approximately once every two months beginning in June 2012 and ending in December 2017 (or January 2018 in the case of the Yukon; exact sampling dates can be found at www.arcticgreatrivers.org) targeting alternate months in alternate years. Width-integrated samples were collected from each river across the hydrograph at sampling locations near the river-mouth but above tidal influence for a total of 194 samples, based on a standardized collection method. Briefly, during open water periods, 1 L surface water samples were collected from stations at each riverbank and 2 L samples were collected from a mid-channel station during all years. All samples were combined in a processing carboy and kept cold. Under-ice samples were collected from the mid-channel surface station through a hole in the ice. Sampling locations were Salekhard (Ob'), Dudinka (Yenisey), Zhigansk (Lena), Cherskiy (Kolyma), Pilot Station (Yukon), and Tsiigehtchic (Mackenzie) (Holmes et al., 2012; McClelland et al., 2008; Raymond et al., 2007; Zolkos et al., 2020).

2.2 DOC concentration, optical properties, and isotopes

Samples for DOC concentration and absorbance measurements were filtered within a few hours of collection through a pre-cleaned Geotech Dispos-a-filter (0.45 μm pore size capsule filter, Geotech Environmental) and frozen until analysis. Concentrations were measured on a Shimadzu TOC/TN analyzer at the Woodwell Climate Research Center (WCRC; formerly Woods Hole Research Center) with values from individual samples reflecting the mean of 3–5 replicate injections (coefficient of variance <2%) (Mann et al., 2016). Absorbance was analyzed on a dual-beam Shimadzu UV-1800

spectrophotometer (200-800 nm at 1 nm intervals; 1 cm pathlength) at WCRC (Mann et al., 2016). Carbon specific ultra-violet absorbance ($SUVA_{254}$; which is correlated with DOC aromaticity) was calculated by dividing the decadic UV absorbance at 254 nm by the DOC concentration of each sample (Weishaar et al., 2003).

Samples for measurements of stable carbon isotope ratios and radiocarbon content were filtered through 47 mm quartz filters (Whatman QM-A 2.2 μm pore size, pre-combusted at 850°C for 6h) and stored frozen in acid-leached polycarbonate bottles. Samples from 2012–2016 were UV-oxidized on a system that directly connected to vacuum lines where CO_2 was captured and cryogenically purified at Yale University (Raymond & Bauer, 2001b). Sample aliquots were placed in clean quartz tubes, acidified with 0.2 mL of ultra-high-purity 40% phosphoric acid, and sparged with nitrogen to remove inorganic carbon. Pure O_2 was added as an oxidant, samples were oxidized with UV, and CO_2 was captured cryogenically on a vacuum line. The resulting purified CO_2 was then analyzed for $\delta^{13}C$ and $\Delta^{14}C$ at the National Ocean Sciences Atomic Mass Spectrometry facility. Samples for 2017–2018 were subject to wet chemical oxidation (Lang et al., 2016) and analyzed for $\delta^{13}C$-DOC and $\Delta^{14}C$-DOC at the accelerator mass spectrometer (AMS) facility at ETH-Zurich. Briefly, sample aliquots were placed in combusted glass vials, and 1 mL acidified sodium persulfate solution was added as an oxidant. Vials were sealed and purged with high-purity helium to remove inorganic carbon. Samples were then heated to 95 °C for 1 hour to convert sample DOC to CO_2 and injected into a MICADAS (MIni CArbon DAting System) accelerator with a gas-accepting ion source (Ruff et al., 2010). All data have been corrected for the processing blanks and standards according to Lang et al., 2016.

2.3 FT-ICR MS analysis

Samples for FT-ICR MS analyses were filtered through pre-cleaned Geotech Dispos-a-filter (0.45 μm pore size capsule filter, Geotech Environmental) into pre-cleaned high-density polyethylene bottles and stored frozen until being solid-phase extracted onto reversed phase BondElut PPL columns (100 mg; Agilent) as previously described (Dittmar et al., 2008). Acidified (pH 2) samples were passed through pre-cleaned PPL columns with volumes adjusted to a target concentration of 40 μg C mL^{-1} in final methanol (JT Baker HPLC grade) elutes. Extracts were stored at -20° C until analysis on a 21 T FT-ICR MS at the National High Magnetic Field Laboratory in Tallahassee, Florida (Hendrickson et al., 2015; Smith, D. F. et al., 2018) with negative electrospray ionization. Each mass spectrum collected consisted of 100 co-added time domain acquisitions.

Molecular formulae were assigned to spectral peaks with >6σ root-mean-square baseline noise (O'Donnell, Aiken, Butler, et al., 2016; Spencer et al., 2019) with PetroOrg ©^{TM} software (Corilo, 2015). Elemental constraints of $C_{1-45}H_{1-92}N_{0-4}O_{1-25}S_{0-2}$ and a mass accuracy ≤300 ppb were applied to formulae assignments (Kellerman et al., 2018). The modified aromaticity index (AI_{mod}) was calculated to assess the degree of aromaticity based on molecular formula (Koch & Dittmar, 2006, 2016). Compound classes were assigned using AI_{mod} and elemental ratios as follows: polyphenolics ($0.5 < AI_{mod} \leq 0.66$); condensed aromatics ($AI_{mod} > 0.66$); highly unsaturated and phenolics (HUPs; $AI_{mod} \leq 0.5$, $H/C < 1.5$, $O/C \leq 0.9$); aliphatic ($1.5 \leq H/C \leq 2.0$, $O/C \leq 0.9$ and $N = 0$); sugar-like ($O/C > 0.9$); and peptide-like ($1.5 \leq H/C \leq 2.0$, and $N > 0$). Though molecular formulae

can be assigned to FT-ICR MS peaks, each molecular formula may represent multiple isomers and therefore exact compound structure cannot be determined. Relative abundances of each formula were determined by normalizing each peak magnitude to the sum of all assigned peaks in each sample. The contributions of the compound classes were then calculated as the sum of all the relative abundances of each peak in each compound class divided by the summed abundances of all assigned formulae in each sample expressed as percentages. Similar calculations were used to determine the relative abundances of compounds containing different elemental compositions (e.g. CHO, CHON, CHOS, CHONS).

2.4 Data analyses

Statistical tests for differences between seasons were performed on both bulk metrics and on FT-ICR MS data using the *rstatix* (Kassambara, Alboukadel 2020*)* and *car* (Fox & Weisberg, 2019) packages and base R (R Core Team, 2019) (see Table S1 for full list of variables and results of statistical tests). Normality was tested using the Shapiro-Wilk test of residuals from the linear model of variable by season. For variables failing the normality test, Kruskal-Wallis tests and Wilcoxon's tests to assess differences between seasons were performed. For variables meeting the normality test, homogeneity of variance was tested using Levene's test. For variables failing the homogeneity of variance test, a one-way ANOVA assuming unequal variance and a pairwise *t*-test to assess differences between seasons was used. For variables that passed the homogeneity of variance, a one-way ANOVA assuming equal variance and a pairwise *t*-test was performed.

Correlations between percent relative abundances (%RA) of individual molecular formulae and bulk metrics of DOM quantity, composition, and age (DOC concentration, $SUVA_{254}$, and Δ^{14}C-DOC values) were examined using Spearman's rank correlation coefficients (Spearman correlation; a non-parametric measure of the strength of two variables' relationship with no distribution assumptions and minimal sensitivity to outliers; significant if $\rho_S \geq 0.2$ and $p < 0.05$). Spearman correlations for each of the 1,328 formulae present in the CARF (which were formulae identified in every sample from every river for all six years, i.e. always present) as well as the 361 formulae present in the "island of stability" (IOS) were calculated between environmental parameters and the sum-normalized intensity of peaks with assigned formulae using R (R Core Team, 2019) using the packages *reshape2* (Wickham, 2007), *vegan* (Oksanen et al., 2019), *Hmisc* (Harrell & Dupont, 2019), and *fields* (Furrer et al., 2017).

Principal component analysis (PCA) was used to examine relationships between DOM compositional data (FT-ICR MS data, DOC concentrations, $SUVA_{254}$, and δ^{13}C-DOC and Δ^{14}C-DOC values) in R (R Core Team, 2019) using the *factoextra* package (Kassambara, Alboukadel & Mundt, 2017) with variables scaled to unit variance to make them comparable. This technique reduces continuous multivariate data dimensionality while retaining information on dataset variability, allowing patterns in dataset organization to emerge.

3. Results and Discussion

3.1 Seasonal synchrony and the latent high-energy spring subsidy

Samples were examined by season, with spring freshet (May and June), summer (July-October) and winter low-flow period (November-April) corresponding to distinct hydrologic phases of high-latitude northern rivers (Holmes et al., 2012). Averaged across the six sampling years, spring freshet had highest DOC concentrations and winter baseflow had the lowest (Table 1; Fig. 2a; Kruskal-Wallis test: $p < 0.0001$; see Table S1 for full test results from statistical tests in this section), as has been shown in past studies of many Arctic rivers where DOC concentrations correlate with discharge and are highest during freshet both in large (e.g. Amon et al., 2012; Kaiser et al., 2017; Mann et al., 2016; Raymond et al., 2007) and smaller (e.g. Johnston et al., 2018; McClelland et al., 2014) Arctic rivers. Average $SUVA_{254}$ values were also highest during spring freshet and lowest in winter (Table 1; Fig. 2b; Kruskal-Wallis test: $p < 0.0001$), as is observed when aromatic terrestrial material is a significant contributor to riverine DOM during Arctic freshet but less of a contributor during frozen winter conditions (Mann et al., 2016; O'Donnell et al., 2012; Striegl et al., 2007). Spring freshet had the lowest δ^{13}C-DOC values averaged across all rivers and years, though individual rivers showed more variability and lacked strong seasonal variation as has been previously demonstrated (Table 1; Fig 2c; Raymond et al., 2007; Wild et al., 2019), with only winter and spring being statistically different from one another (Wilcoxan's pairwise comparisons: $p_{adj} < 0.05$). Spring freshet also had the highest Δ^{14}C-DOC values, while winter baseflow had the lowest values (radiocarbon ages from 1533 years before present (ybp) to >modern and 2371 ybp to >modern, respectively; Table 1; Fig. 2d; Kruskal-Wallis test: $p < 0.0001$). This pattern of modern DOC during spring freshet and older DOC during winter has been well documented previously for large Arctic rivers (Raymond et al., 2007; Wild

et al., 2019), though some aged DOC has been seen in spring in large Arctic rivers as well (Schwab et al., 2020).

The FT-ICR MS compound classes comprised of condensed aromatics and polyphenolics (Table 2; Fig. 2e-f) have been tied to allochthonous DOM inputs from soil and vascular plants, and had their highest average %RA during the spring freshet and lowest average %RA during winter across all samples (Kruskal-Wallis test: $p < 0.0001$; one-way ANOVA: $p < 0.0001$, respectively) (Johnston et al., 2019; Kellerman et al., 2018; O'Donnell, Aiken, Butler, et al., 2016; Seidel et al., 2015; Sleighter & Hatcher, 2008). Some condensed aromatics may also originate from combustion, which can be a substantial aerosol source in the Arctic (Barrett et al., 2015). Average %RA of sugar-like formulae across all samples was also highest during spring freshet and lowest in winter (Table 2; Fig 2g; Kruskal-Wallis test: $p < 0.0001$). Both the contribution of sugar-like formulae to DOM and the concentration of total hydrolysable neutral sugars in Arctic rivers have been shown to correspond to high-discharge events, suggesting that sugar-like formulae may build up in soils over winter and then be disproportionately flushed from land to river in surface runoff (Johnston et al., 2018; Kaiser et al., 2017).

In contrast, winter contained the greatest contribution of HUPs while spring freshet contained the smallest (Table 2; Fig. 2h; Kruskal-Wallis test: $p < 0.0001$), though HUPs dominated all samples' %RA as is typical in DOM globally (Kellerman et al., 2018; McDonough, O'Carroll, et al., 2020; Spencer et al., 2019). HUPs have been attributed to vascular plant–derived lignin degradation products or chemically persistent aquatic carboxyl rich alicyclic molecules (CRAM), with debate over whether these different sources can be distinguished using FT-ICR MS data (Sleighter & Hatcher,

2008). CRAM in turn has been attributed to biomolecules of microbial origin, suggesting some HUPs could be autochthonously derived (Hertkorn et al., 2006). Winter also contained the largest average %RA of the core Arctic riverine fingerprint and island of stability formulae (CARF and IOS; see section 3.2; Figure 2i-j; Table 2; Kruskal-Wallis test: $p < 0.001$ and one-way ANOVA: $p < 0.0001$, respectively). The aliphatic and peptide-like compound classes (which make up on average <1 %RA for all seasons and all rivers) show less clear seasonal variation (Table 2; pairwise *t*-test $p_{adj} < 0.05$ for spring/summer and summer/winter only, and Kruskal-Wallis test: $p = 0.15$, respectively). This is likely due to the fact that aliphatics have been shown to derive from a wide variety of sources that may differ spatially and seasonally around the Arctic, including vegetation (Johnston et al., 2019), permafrost inputs (Stubbins et al., 2017), and microbial production in glaciers and snow (Antony et al., 2017; Feng et al., 2016). In general, peptide-like formulae also provide evidence for microbial activity (Antony et al., 2017; Lawson et al., 2014).

Past studies have suggested that dramatic seasonal variations dominate patterns in Arctic riverine DOM composition, despite watershed specific characteristics, with winter DOM being most chemically distinct compared to spring or summer DOM (Amon et al., 2012; Holmes et al., 2012; O'Donnell et al., 2012). The pan-Arctic similarity in DOM composition in the present study confirmed this seasonal dominance: principal component one (PC1) of the PCA (Fig. 3; see Fig. S1 for variable contributions to PC1 and PC2) separated the samples by seasonality and explained 39.82% of the variance, while PC2 only accounted for 17.36% of the variance (the watershed-specific drivers of PC2, including watershed percent permafrost coverage, are discussed in section 3.4).

Characteristics indicative of recently produced terrestrial DOM such as ^{14}C enrichment (Amon et al., 2012; Hood et al., 2009), ^{13}C depletion (Fellman et al., 2014; Raymond & Bauer, 2001a), increased relative abundances of condensed aromatic and polyphenolic formulae (Behnke et al., 2020; Kellerman et al., 2014; Seidel et al., 2015), elevated DOC concentration (Tank et al., 2018) and elevated $SUVA_{254}$ values (Fellman et al., 2008) clustered on the negative end of PC1 (Fig. 3a), as did samples from spring freshet (Fig. 3b). The positive end of PC1 was associated with winter samples (Fig. 3b), as well as with ^{14}C depletion and ^{13}C enrichment (previously associated with groundwater DOM; Fig 3a) (McDonough, Rutlidge, et al., 2020; Nakata et al., 2013; Schiff et al., 1997). Increased terrestrial DOM signatures are characteristic of Arctic freshet, with deep, sub- and intra-permafrost groundwater representative of winter baseflow in perennially flowing Arctic rivers (Amon et al., 2012; Douglas et al., 2013; Holmes et al., 2012; Johnston et al., 2018; Mann et al., 2016; Woo et al., 2008).

Despite the overwhelming terrestrial and aromatic nature of Arctic freshet DOM (Amon et al., 2012; Holmes et al., 2012; Johnston et al., 2018; Mann et al., 2016), Arctic riverine DOM has also been found to be most bioavailable during freshet (Holmes et al., 2008). Because aromatic DOM is usually considered less bioavailable than aliphatic DOM (D'Andrilli et al., 2015; O'Donnell, Aiken, Butler, et al., 2016; Textor et al., 2019; Ward & Cory, 2015), this freshet combination of highly aromatic terrestrial bulk signature yet apparently bioavailable DOC pool poses a chemical paradox. The high degree of chemical resolution afforded by FT-ICR MS presents a solution by identifying a latent high-energy subsidy present concurrently with the bulk of more oxidized and aromatic “terrestrial” formulae that dominate the spring freshet DOM. Unique molecular

fingerprints of spring freshet (Fig. 4a), summer (Fig. 4b), and winter (Fig. 4c) riverine DOM were identified as formulae only present during one season in at least three samples and two rivers (Table S2; Table S3). A suite of unique aliphatic and peptide-like formulae distinguished the spring fingerprint, demonstrating an energy-rich spring subsidy. These formulae have higher H/C ratios (and thus greater stored chemical energy) than the unique winter aliphatic and peptide-like formulae identified. The high H/C ratios of such formulae likely correspond to energy-rich compounds (Hopkinson et al., 1998; Lawson et al., 2014; Smith, H. J. et al., 2018; Spencer et al., 2015), as do the unique sugar-like formulae present, which can be rapidly and preferentially consumed by microbes (O'Donnell, Aiken, Butler, et al., 2016; Spencer et al., 2015).

Compound class trends corroborate the concept of an energy-rich spring subsidy. Five rivers had the highest average %RA of sugar-like formulae during freshet while four had the greatest contribution of aliphatic and peptide-like formulae during freshet (Table 2). In contrast, the mean of the weighted averages of the H/C ratios for all molecular formulae present in each sample was primarily lowest in spring and highest in winter (and mean O/C weighted average the opposite; one-way ANOVA: $p < 0.0001$ and Kruskal-Wallis test: $p < 0.0001$, respectively; Fig. 2k-l for dataset averages; Table S1 for statistics; Table S4 for river averages). This shows that bulk freshet DOM metrics (e.g. averaged elemental ratios) are dominated by oxidized, aromatic material despite the presence of a latent high-energy fraction. In previous Arctic river studies, both the terrestrial signature of DOM (%RA of polyphenolics and carbon normalized lignin yield) and %RA of sugar-like formulae increased during freshet on a medium-sized Russian river (Johnston et al., 2018). Further, carbohydrates, amino acids, and plant phenols have

been observed to increase in spring indicating both an increase in high-energy compounds and direct terrestrial leaching (Kaiser et al., 2017). The persistence of energy-rich formulae near river mouths in spring shows that low temperature, rapid flow conditions in freshet facilitate leaching and rapid downstream shunting of energy-rich, biolabile compounds (Raymond et al., 2016), while also mobilizing the aromatic compounds that provide the bulk terrestrial DOM signature. The unique spring formulae may represent a bioavailable subsidy to marine microbial communities during a time when both discharge and DOC concentrations are at their peak.

The unique molecular formulae present in winter (the largest unique seasonal set of formulae present) contained HUPs and a suite of unique peptide-like and aliphatic formulae, which may reflect microbial inputs (Antony et al., 2017; Lawson et al., 2014). These may be derived from microbial degradation that occurs during the subsurface flow of groundwater and could persist into main river channels without being consumed during winter due to cold under-ice conditions despite their hypothesized biolabile nature (Lawson et al., 2014; Textor et al., 2019; Wickland et al., 2012). Additionally, the concentrations of DOC in winter in these rivers may be too low to make individual formulae metabolically worthwhile for microbial consumption despite their theoretically biolabile composition, as has been suggested in deep ocean DOC (Arrieta et al., 2015).

3.2 Radiocarbon ages and potential groundwater sources of winter DOC

The Δ^{14}C-DOC values of the winter samples also suggest inputs of moderately aged carbon from soil sources carried by groundwater inputs (which can drive baseflows in Arctic rivers; e.g. Clark et al., 2001; Douglas et al., 2013; Walvoord & Striegl, 2007).

A discussion of groundwater in the permafrost zone is complicated by extreme variability in both permafrost extent and groundwater flowpaths around the pan-Arctic (Walvoord & Kurylyk, 2016; Woo et al., 2008). Permafrost often serves as an aquatard due to ice saturation in soils, leading to perched water tables above an impermeable surface. Subsurface flow of water in permafrost zones is complex; water can be located above the permafrost surface (suprapermafrost groundwater), below the permafrost layer (subpermafrost groundwater), or inside unfrozen zones within permafrost (taliks; intrapermafrost groundwater) (Woo, 2012). Here the term groundwater indicates all of these, though differences in their contributions will also be discussed.

The oldest DOC in this dataset ($\Delta^{14}C$ -262‰) occurred in the winter Ob' samples. Across the six rivers winter had significantly lower $\Delta^{14}C$ values (mean ± standard error: -50.23 ± 6.89‰) than spring (6.35 ± 11.27‰; Wilcoxon's test: $p_{adj} < 0.0001$) and insignificantly lower values than summer (-30.76 ± 5.90‰ Wilcoxon's test: $p_{adj} = 0.13$) (Fig. 2d; Table S1). Since the Ob' watershed contains the least continuous permafrost of the six rivers (Holmes et al., 2012), it likely receives the most input from deep subpermafrost/intrapermafrost groundwaters (which are most connected to surface waters when not blocked by impermeable continuous permafrost layers; Walvoord & Kurylyk, 2016). Discontinuous permafrost allows subpermafrost groundwater to provide winter baseflow when other sources of river water are limited due to frozen surface conditions (Douglas et al., 2013; Walvoord et al., 2012). These wintertime groundwater inputs likely carry aged DOC, since DOC that persists in deep groundwater globally generally carries an aged signature (McDonough, Rutlidge, et al., 2020; Nakata et al., 2013; Schiff et al., 1997; Tipping et al., 2010; Wassenaar et al., 1991), and since unfrozen suprapermafrost

groundwater flowing during winter months moves through taliks or deeper active layer soils which generally store older carbon and take longer to freeze up (Wild et al., 2019).

Thawing permafrost may contribute to the moderately aged groundwater DOC found in these rivers during the winter, but at present DOC ages in this water are not old enough to clearly distinguish between organic matter contributions from unfrozen surface soils or Holocene permafrost or peat deposits ($\Delta^{14}C$ values of -197.5 ± 148.3 versus -567.5 ± 156.7‰ for Eurasia; Wild et al., 2019). What these data do indicate is that at present, DOC contributions from older permafrost are minimal, which is consistent with small contributions of old permafrost carbon to stream DOC identified in isotopic mixing models (Mann et al., 2015; O'Donnell et al., 2019). While permafrost $\Delta^{14}C$-DOC values can be highly ^{14}C-depleted, for example reaching $\Delta^{14}C$ values below -950‰ in some locations (Mann et al., 2015; Spencer et al., 2015; Vonk et al., 2013; Wild et al., 2019), mainstem Arctic rivers generally exhibit higher $\Delta^{14}C$-DOC values (Amon et al., 2012; Neff et al., 2006; Raymond et al., 2007; Wild et al., 2019). Modern radiocarbon ages have even been observed directly adjacent to permafrost thaw slumps (Spencer et al., 2015; Stubbins et al., 2017). This lack of clear permafrost thaw signature is consistent with other studies of large Arctic rivers, which have also failed to observe an unambiguous molecular or isotopic fingerprint of thawed permafrost DOC (Drake, Guillemette, et al., 2018; Mann et al., 2015; Spencer et al., 2015; Wild et al., 2019). Instead, the moderately aged $\Delta^{14}C$-DOC values occurring in the rivers during winter are within the range of expected contributions from both suprapermafrost groundwater as it is forced through deeper active layer channels during freeze-up (e.g. Connolly et al., 2020;

Wild et al., 2019), and from deeper groundwater aquifers (e.g. McDonough, Santos, et al., 2020; Wassenaar et al., 1991).

3.3 Core Arctic riverine fingerprint: a stable terrestrial DOM source to the global ocean?

The CARF (1,328 formulae) were identified as the formulae present in all samples (all rivers and years; Fig. 5a; Table S2; Table S5) and made up the bulk of the relative abundance (%RA, or signal intensity) across DOM samples (>60%). The compositional space occupied by the CARF reflects a wide variety of compound classes, including those with probable terrestrial sources such as polyphenolics and condensed aromatics (Behnke et al., 2020; Kellerman et al., 2018; Seidel et al., 2015; Sleighter & Hatcher, 2008) and those with possible autochthonous sources such as aliphatics and sugar-like formulae (Antony et al., 2017; Feng et al., 2016; Johnston et al., 2018). The CARF is similar to the common formulae identified in all samples along a transect of the Ob'-Irtysh river system and contained a similar number of formulae in a comparable central region of van Krevelen space (1,328 versus 1,629 formulae, respectively), suggesting that the CARF could appear throughout the upstream extents of large Arctic rivers as well as near their termini (Perminova et al., 2019).

The prevalence of the CARF reveals that at all times of year, all of these large Arctic watersheds produce a chemically diverse yet ubiquitous compositional signal that dominates riverine DOM flux to the Arctic Ocean. The persistence of this signal into the global ocean depends on the long-term compositional stability of the CARF, which is at present unknown. However, the CARF includes 284 (79%) of 361 formulae previously identified as the island of stability (IOS), a narrow compositional range associated with

^{14}C-depleted DOC in the ocean (Fig. 5b; Table S2) (Lechtenfeld et al., 2014). Lechtenfeld et al. (2014) proposed the IOS represents the end products of DOM degradation, featuring formulae of chemically stable molecules produced after biological and physical DOM processing. The percent relative abundance of the IOS present in DOM increased with increasing DOC age in a global sample set including riverine, lake, groundwater and marine DOM, demonstrating the persistence of the IOS across the aquatic continuum and suggesting its chemical stability leads to its old radiocarbon age (Kellerman et al., 2018).

All IOS formulae were identified in at least one river in this dataset. The mean relative abundance of IOS formulae in each sample increased significantly (Table S1; one-way ANOVA: $p < 0.0001$) from freshet (25.4 ± 0.6%) to summer (28.2 ± 0.3%) to winter (29.9 ± 0.3%) (Fig. 2j). The mean number of IOS formulae present in each season was largely invariant (spring: 347 ± 2; summer: 351 ± 1; winter: 351 ± 1), only increasing significantly between spring and winter (Table S1; Wilcoxon's test: $p < 0.05$), and the total number of molecular formulae did not change significantly across season (Table S1; Kruskal-Wallis test: $p = 0.79$). Thus, the increase in IOS contribution across seasons is likely due to the increasing relative abundance of the IOS formulae present in each sample spectrum, suggesting the primary sources of the IOS are present year-round and most influential during winter baseflow. Supra- and subpermafrost groundwater inputs have been shown to drive baseflow in both lower latitude Arctic rivers on discontinuous permafrost (Boucher & Carey, 2010; Douglas et al., 2013) and higher latitude Arctic rivers (Blaen et al., 2014; Bolduc et al., 2018; Woo et al., 2008; Yoshikawa et al., 2007), especially in winter for watersheds that do not freeze solid

(Clark et al., 2001; Pollard, 2005). These results align with a global survey that showed groundwater from a Colorado aquifer contained 36% relative abundance IOS (Kellerman et al., 2018), and suggest groundwater is an IOS source here as well.

Groundwater inputs also provide the stable winter baseflow present in the great Arctic watersheds, which span high and mid-latitudes. Despite being completely underlain with continuous permafrost, the Kolyma watershed receives groundwater inputs year round, and its winter flow is sourced entirely from supra- and subpermafrost groundwater (Glotov et al., 2015). Similarly, winter discharge from spring systems in the middle basin of the Lena River Basin are thought to consist of deep intrapermafrost groundwater (Hiyama et al., 2013). Discontinuous permafrost allows even greater groundwater connectivity; in the Yukon watershed (23% continuous permafrost), weathering signatures have shown that inputs from deep groundwater flowpaths dominated during winter but were present in small amounts throughout the year (Douglas et al., 2013), and long-term increases in groundwater contribution to streamflow have been attributed to deepening flowpaths caused by permafrost degradation (Walvoord & Striegl, 2007). In the Ob', where continuous permafrost coverage is low but sporadic and discontinuous permafrost underlie a quarter of the watershed, groundwater reservoirs join other water sources such as lakes and wetlands in providing baseflow during winter and provide the bulk of solute inputs in its lower latitude, non-permafrost impacted reaches (Frey et al., 2007; Xu et al., 2020).

Given the role that supra-, intra-, and sub-permafrost groundwater play in large Arctic river baseflow, DOM from these groundwater sources likely provides part of the unifying backbone of the CARF and IOS compositions which persist during all periods of

the hydrograph, and onto which spring and summer seasonal signals are superimposed. In general, DOC present in deep groundwater aquifers is stable enough to have persisted without further degradation, leading to generally old radiocarbon ages and low concentrations particularly at depth (McDonough, Rutlidge, et al., 2020; McDonough, Santos, et al., 2020; Nakata et al., 2013; Pabich et al., 2001; Schiff et al., 1997). It is thus not surprising that winter baseflow sourced from groundwater (particularly subpermafrost) contributes stable formulae to large Arctic rivers.

By definition, formulae present in the CARF that had positive Spearman correlations with DOC concentration (Fig. 6a), $SUVA_{254}$ (Fig. 6b), and ^{14}C enrichment (Fig.6c) (and the smaller subset of positively correlated IOS formulae; Fig. 6d-f) had their highest relative abundances in samples that were taken when DOM was prevalent, aromatic, and young. These CARF formulae are likely sourced from recent plant matter rather than from the groundwater contribution to the CARF addressed above, since these formulae have their highest relative abundances during spring freshet when DOC is abundant and ^{14}C-enriched (Holmes et al., 2012; Raymond et al., 2007) and when terrestrial polyphenolic and condensed aromatic formulae (Kellerman et al., 2014; Seidel et al., 2015) and formulae with high O/C ratios dominate. Formulae negatively correlating with $\Delta^{14}C$-DOC, $SUVA_{254}$, and DOC in the CARF align with and include the negatively correlated IOS region (the bulk of the IOS), which resembles a compositional region previously correlated to old groundwater DOC (McDonough, Rutlidge, et al., 2020). Low DOC concentrations (McDonough, Santos, et al., 2020), depleted $\Delta^{14}C$-DOC values (McDonough, Rutlidge, et al., 2020; Schiff et al., 1997), and low $SUVA_{254}$ values (Chapelle et al., 2016; O'Donnell et al., 2012) are often found in deep groundwater

aquifers, suggesting the association of these traits with the IOS signal and this subset of the CARF's signature in these rivers is consistent with a subpermafrost groundwater source.

The positively and negatively correlated regions in the CARF may be indicative of both the different sources and fates of CARF DOM. The negatively correlated, old, IOS-like region is consistent with subpermafrost groundwater and likely persists into the global ocean due to its chemical stability. The positively correlated, modern edges of the CARF (dominated by more aromatic and plant-derived compounds) are primarily sourced from terrestrial (vegetation- and soil-derived) DOM which may persist through the winter via shallower groundwater inputs. Despite the fact CARF formulae persist as far as the mainstem rivers, they may eventually degrade once they enter the ocean. The greater oxidation and aromaticity of most of the positively correlated formulae may render them more susceptible to photochemical degradation and flocculation (Kujawinski et al., 2004; Massicotte et al., 2017; Spencer et al., 2007; Stubbins & Dittmar, 2015) than are the more centrally located formulae, while the small set of positively correlated higher H/C compounds with more aliphatic nature may be more susceptible to eventual microbial processing (Lawson et al., 2014; Smith, H. J. et al., 2018). At whatever rate these processes occur, the result would be an eventual distillation of the terrestrial DOM signal in the ocean, with a final resemblance to the IOS, demonstrating that the stable oceanic carbon pool represented by the IOS (the original sources of which are unknown; Kellerman et al., 2018; Lechtenfeld et al., 2014) could have a riverine source.

The pan-Arctic watershed is a major source of terrestrial DOM to the global ocean, with 10–16% of Arctic river DOM potentially entrained in North Atlantic Deep

Water formation and increasing degradation of Arctic terrestrial DOM in transit from the Arctic to Atlantic to Pacific Oceans (Hernes & Benner, 2006). It remains to be seen how ubiquitous the CARF signal is in rivers globally (and whether it should more accurately be known as the core riverine fingerprint), but the CARF's ubiquity in large Arctic rivers combined with the persistence of Arctic riverine DOM well into the Arctic Ocean (Amon & Meon, 2004; Guéguen et al., 2005) could make the non-IOS portion of the CARF a future molecular tracer of riverine input within the Arctic Ocean Basin. In turn, the contribution of the IOS to Arctic riverine DOM was large (~20–30 %RA for all samples; Table 2) compared to the IOS contribution previously reported for rivers and streams in a global dataset (11–22 %RA). The CARF's encapsulation of the IOS and the significant contribution of IOS to Arctic riverine DOM suggest that Arctic rivers could be one source of IOS formulae and stable DOM to the global ocean, potentially contributing to the ocean's carbon sink of stable DOM (Jiao et al., 2010).

3.4 Permafrost extent modifies riverine DOM

Principal component two (PC2) of the PCA examining DOM sample variability (Fig. 3; Fig. S1) separated by watershed. Heteroatom (nitrogen or sulfur)-containing classes and aliphatics clustered at the positive end, which corresponded with Ob' samples (~2% continuous permafrost). Kolyma and Lena samples (~100% and ~77% continuous permafrost, respectively) cluster at the negative end, while the Yenisey, Yukon, and Mackenzie (~33%, ~23%, and ~16% continuous permafrost, respectively) spread between. High heteroatom content and aliphatics contribution have been correlated with microbial processes in many environments including snow (Antony et al., 2017), oceans

(Bayer et al., 2019; Zheng et al., 2019), and lakes (Kellerman et al., 2018), suggesting that different contributions of microbially-derived DOM rich in heteroatoms may drive the separation along PC2 by watershed. Microbially-derived DOM is more dominant in aquatic environments with longer residence times (Hodgkins et al., 2016; Kellerman et al., 2014; Kellerman et al., 2015). It is well documented that permafrost extent influences water residence time in catchments and soils (Ala-Aho et al., 2018; Song et al., 2020; Walvoord & Kurylyk, 2016); permafrost creates shallow aquatards, routing water rapidly through porous organic soil layers to streams (Tetzlaff et al., 2015; Woo et al., 2008). Permafrost thaw leads to deeper active layers (which route water through deeper, less permeable soil, increasing subsurface water residence times), expanding taliks (which increase connections between subpermafrost groundwater and surface waters and provide new subsurface flow paths), and abrupt thaw processes like thermokarst (which in the short term can release a transient pulse of freshly thawed DOM and in the mid- to long term can change water storage and increase talik formation) (Bring et al., 2016; Tetzlaff et al., 2015; Walvoord & Kurylyk, 2016; Walvoord et al., 2012; Woo et al., 2008). These expanded groundwater flowpaths can allow for greater microbial DOM processing, which in turn can yield heteroatom-rich DOM (Antony et al., 2017; Bayer et al., 2019; Kellerman et al., 2018; Musilova et al., 2017; Smith, H. J. et al., 2017; Spencer et al., 2014; Zheng et al., 2019).

In Sweden (Hodgkins et al., 2016), Russia (Gandois et al., 2019), and the Canadian Arctic (Fouché et al., 2017), waters draining permafrost thaw (i.e., thermokarst) features have shown greater contributions of heteroatom-containing formulae and/or microbial DOM than waters draining less degraded permafrost landscapes, suggesting the

increasing importance of microbial DOM sources with increasing water residence time and flow depth in soils due to thaw. Fundamentally, differences in type and extent of permafrost impact hydrology and DOM chemistry (MacDonald et al, 2021; O'Donnell, Aiken, Swanson, et al., 2016). The six watersheds in this study encompass a continuum of types of surface-groundwater connectivity. These range from substantial opportunity for deep/subpermafrost groundwater inputs with long subsurface residence time in the permafrost-free upper reaches of the Ob' to limited subpermafrost groundwater inputs and substantial suprapermafrost groundwater inputs in the continuous permafrost of the Kolyma (Frey et al., 2007; Glotov et al., 2015). Due to the evidence for microbially-derived heteroatom-rich DOM, it appears likely the separation on PC2 is caused by varying permafrost extent, flow paths, and subsurface water residence times in the study watersheds and the subsequent differing contributions of degraded DOM sources.

3.5 Future Arctic change: Shifting DOM sources and subsidies

Our work presents the longest time series of FT-ICR MS DOM data yet conducted and combines these data with comprehensive DOC isotopic data to illuminate the controls on Arctic riverine DOM composition and export. Climate change may have significant repercussions for the primary controls presented here such as seasonality and permafrost extent (summarized in Fig. 7). At present, there is seasonal synchrony in DOM composition amongst the large pan-Arctic rivers, with the oldest and most microbially processed DOM being transported in winter and a latent subset of DOM serving as a high-energy subsidy in spring. Thus, our ultra-high resolution molecular data help explain the historical paradox of Arctic freshet DOM both being biolabile and

having a bulk terrestrial signature. Arctic rivers may currently be a significant source of stable DOM to the global ocean through the IOS, which is highly abundant in these rivers, and the non-IOS portions of the CARF may prove a useful tracer of riverine DOM in the Arctic Ocean. Permafrost extent currently appears to control the heteroatom content of DOM though groundwater flowpaths and microbial degradation. While the Arctic system is complex and warming will likely cause a variety of unforeseen impacts on DOM composition, based on the current controls on DOM composition in Arctic rivers we postulate the following three major changes are likely to occur:

1. *Changing freshet hydrographs could modify timing and magnitude of the spring high-energy DOM subsidy to the Arctic Ocean:* River discharge to the Arctic Ocean has been increasing throughout the past century (Bring et al., 2016; Durocher et al., 2019; McClelland et al., 2006; Peterson et al., 2002) with models projecting increases continuing well into the next century (Arnell, 2005; Rawlins et al., 2010; Walsh et al., 2005). A recent analysis of 30 years of daily discharge of the Ob', Yenisey, Lena, and Mackenzie revealed a shift towards earlier spring freshet timing and a general flattening of the Arctic riverine hydrograph (Ahmed et al., 2020). This flattening is due in part to increases in the proportion of annual discharge occurring during winter and concomitant decreases in proportion of annual discharge occurring during freshet. This leads to an overall greater annual riverine discharge with a broader-based hydrograph and thus a reduced hydrographic dominance of freshet (Ahmed et al., 2020; Prowse et al., 2006). The influence of changing discharge regimes will be felt in the Arctic Ocean; increasing freshwater inputs will be a primary impact of climate change on near-shore and estuarine

environments (Carmack et al., 2016; Prowse et al., 2006), though the sign and magnitude of actual changes in oceanic production remain uncertain due to the multiple interactions and scales in question (Lique et al., 2016). Species shifts due to freshening and increasing delivery of organic material are likely to occur, with the potential to change the biogeochemistry and primary productivity of the region with possible increases in production due to enhanced nutrient and organic matter flux (Prowse et al., 2006) or decreases in production due to stratification (Carmack et al., 2016). A portion of terrestrial DOM is available for secondary production by marine microbial communities (Letscher et al., 2011), with isotopic studies showing that terrestrial organic matter makes its way into nearshore and offshore marine organisms (Bell et al., 2016; Casper et al., 2015; Dunton et al., 2012; Dunton et al., 2006). Future disconnects between the timing of sea ice melt and riverine freshet with its latent high-energy DOM subsidy (which will likely occur earlier in the year) and the timing of daylight availability (which will remain the same) may lead to disproportionate increases in respiration compared to photosynthesis with carbon routed rapidly to the atmosphere, or to novel situations for oceanic production. The new combination of conditions in the Arctic Ocean that could result may parallel the no-analog communities proposed to occur in regions experiencing novel future climates where new conditions are not comparable to current conditions elsewhere on the globe and where it is thus difficult to anticipate the ecological impacts of current change (Williams & Jackson, 2007).

2. *If permafrost thaw increases groundwater discharge, stable DOM/IOS export to the global ocean may also increase:* Permafrost degradation and thaw increases groundwater

discharge, shifting flow in permafrost-covered watersheds from surface to deeper flow paths and impacting groundwater inputs to streamflow (Song et al., 2020; Walvoord & Kurylyk, 2016; Walvoord et al., 2012). Warming may thus increase subsurface water residence times (Ala-Aho et al., 2018), alter the flux of water and dissolved constituents to Arctic rivers (Song et al., 2020), and increase baseflow (Smith, L. C. et al., 2007; Woo et al., 2008). Such changes are occurring both in watersheds with high watershed percent permafrost coverage (Song et al., 2020) but also in permafrost-free zones as decreasing seasonal soil freezing causes increased hydrologic connectivity (Smith, L. C. et al., 2007). Because the stable IOS and CARF compositional regions appear to be in large part sourced from groundwater, increasing groundwater contributions to river flow may increase the export of stable DOM, contributing to the carbon sink of the stable DOM pool in the global ocean (Jiao et al., 2010).

3. *Permafrost degradation may lead to a greater importance of heteroatom-containing DOM in Arctic rivers:* As outlined in point two above, climate change has the potential to increase the contribution of subpermafrost groundwater to Arctic riverine discharge through permafrost degradation (Smith, L. C. et al., 2007; Song et al., 2020; Walvoord & Kurylyk, 2016; Walvoord et al., 2012). Subsequent increasing subsurface water residence times and increasing flow path options (Tetzlaff et al., 2015; Woo et al., 2008) may lead to increasing microbial production of heteroatom-rich DOM (Antony et al., 2017; Bayer et al., 2019; Kellerman et al., 2018; Musilova et al., 2017; Smith, H. J. et al., 2017; Spencer et al., 2014; Zheng et al., 2019) as has already been demonstrated in degraded permafrost catchments (Fouché et al., 2017; Gandois et al., 2019; Hodgkins et al., 2016).

It appears likely that groundwater-sourced DOM rich in heteroatoms from microbial processing will increase in importance in Arctic rivers, with as-yet-unforeseen consequences to riverine and Arctic Ocean biogeochemistry. Such potentially wide-reaching impacts highlight the importance of riverine DOM composition and export to the biogeochemistry of a changing world.

Acknowledgements:

This work was supported by the National Science Foundation through grants for the Arctic Great Rivers Observatory II (110774), III (WCRC: 1602615; FSU: 1603149; UT: 1602680), and IV (WCRC: 1913888; FSU: 1914081; UT: 1914215) as well as an NSF Graduate Research Fellowship to MIB. A portion of this work was performed at the National High Magnetic Field Laboratory ICR User Facility, which is supported by the National Science Foundation Division of Chemistry through DMR-1644779 and the State of Florida. The authors thank all the helpful researchers at the NHMFL ICR Program who enabled data acquisition and processing. Support was also provided by the South Russian Regional Centre for Preparation and Implementation of International Projects (Ob', Lena, and Yenisey), Northeast Science Station (Kolyma), Yukon River Inter Tribal Watershed Council (Yukon), and Les Kutny and the Aurora Research Institute (Mackenzie). All data used in this paper are freely available on the Open Science Framework (https://osf.io/4azm8/; DOI 10.17605/OSF.IO/4AZM8) and at www.arcticgreatrivers.org/data.

Figure Captions:

Figure 1. Arctic Great Rivers Observatory map. Red dots show sampling locations in this study (Ob' at Salekhard, Yenisey at Dudinka, Lena at Zhigansk, Kolyma at Cherskiy, Yukon at Pilot Station, Mackenzie at Tsiigehtchic or Inuvik). Sampling occurred close to the mouths of the rivers to facilitate integration of whole watershed samples, but above tidal influence. The bold red line shows the boundary of the 16.8×10^6 km^2 pan-Arctic watershed draining into the Arctic Ocean (of which these six rivers cover ~67%).

Figure 2. Descriptive box plots showing seasonal spread of a) DOC, b) specific ultraviolet absorbance at 254 nm ($SUVA_{254}$), c) δ^{13}C-DOC, d) Δ^{14}C-DOC, e) condensed aromatics, f) polyphenolics, g) sugar-like formulae, h) highly unsaturated and phenolics (HUPs), i) core Arctic riverine fingerprint (CARF) contribution, j) island of stability (IOS) contribution, k) mean H/C ratio weighted averages, and l) mean O/C ratio weighted averages for the entire dataset. Median values are shown as dark horizontal lines, boxes represent interquartile ranges, whiskers are 1.5 the interquartile ranges (or minimum/maximum values if no outliers), and dots are outliers. See Supplementary Table 1 for statistical differences between seasons.

Figure 3. a) Loadings for principal component analysis (PCA) of FT-ICR MS compound and heteroatomic classes, specific ultraviolet absorbance at 254 nm ($SUVA_{254}$), dissolved organic carbon (DOC) concentrations, δ^{13}C- and Δ^{14}C-DOC values. b) Each point on the PCA represents a sampling event. Points are colored by river and shaped by season.

Figure 4. Unique molecular formulae identified in at least two rivers and at least three samples for a) spring, b) summer, and c) winter. Each point is a molecular formula.

Figure 5. Molecular fingerprints of pan-Arctic DOM. a) The core Arctic riverine fingerprint (CARF), and b) the island of stability (IOS) present in all samples. Each point is a molecular formula.

Figure 6. Molecular associations between individual formulae and bulk characteristics for the core Arctic riverine fingerprint (CARF) (a-c) and the island of stability (IOS) (d-f). Significant Spearman rank coefficients (absolute-value Spearman's rank correlation coefficient; $\rho_S \geq 0.2$; $p < 0.05$) between molecular formulae and a/d) DOC concentration (705 formulae/54% CARF; 196 formulae/54% IOS), b/d) $SUVA_{254}$ (741 formulae/55%; 191 formulae/53% IOS), and c/f) Δ^{14}C-DOC values (717 formulae/52% CARF; 208 formulae/58% IOS). The color scale indicates correlations between individual molecular formulae intensity and each variable, with darker colors signifying greater absolute value of Spearman rank coefficients (red, positive; blue, negative).

Figure 7. Conceptual sketch of the current controls on DOM composition for discontinous/degraded permafrost (top) and continous permafrost (bottom). Seasonality alligns with PC1 of the PCA (Fig. 3), with spring freshet on the left and winter baseflow conditions on the right. The path of summer flow through the deepening active layer is also shown. Spring is dominated by aromatic DOM from terrestrial sources (orange

hexagons), with a small contribution of high-energy compounds (red triangles) that are bioavailable to heterotrophic microbes (green pacman). Groundwater flow occurs yearround but is undiluted and thus dominant during winter baseflow and produces microbially altered heteroatomic-rich and older DOM (yellow circles). Hydrologic flow connection due to permafrost extent alligns with PC2, with continous permafrost on the bottom and discontinous/degraded permafrost on the top. In regions of continuous permafrost, groundwater contribution to streams is small and flow paths limited. Permafrost degradation leads to greater groundwater contributions, more flow path possibilities and longer residence time, and a greater impact of groundwater DOM from autochtonous production or permafrost-thaw.

Tables:

Table 1. Total dissolved organic carbon (DOC) concentrations, specific ultraviolet absorbance at 254 nm ($SUVA_{254}$), and carbon isotope values across the six great Arctic Rivers from June 2012 to December 2017 (or January 2018 for the Yukon) (mean ± standard error) during spring (May and June), summer (July-October), and winter (November-April).

River	Season	DOC $mgCL^{-1}$	$SUVA_{254}$ $Lmg\ C^{-1}m^{-1}$	δ^{13}C-DOC (‰)	Δ^{14}C-DOC (‰)
Ob’	Spring	11.7 ± 0.9	3.7 ± 0.2	-28.7 ± 0.4	23.0 ± 7.0
	Summer	11.0 ± 1.0	3.5 ± 0.2	-28.1 ± 0.5	-32.8 ± 12.9
	Winter	7.6 ± 0.6	3.2 ± 0.2	-28.5 ± 0.5	-94.8 ± 20.1
Yenisey	Spring	7.8 ± 1.7	3.5 ± 0.3	-27.8 ± 1.0	-6.3 ± 41.2
	Summer	5.5 ± 0.5	3.3 ± 0.1	-27.4 ± 0.7	-28.8 ± 13.9
	Winter	3.3 ± 0.2	2.7 ± 0.1	-26.9 ± 1.0	-45.4 ± 6.0
Lena	Spring	12.5 ± 3.0	3.5 ± 0.2	-28.8 ± 0.5	47.6 ± 12.1
	Summer	7.1 ± 0.5	3.1 ± 0.2	-27.9 ± 0.2	20.5 ± 5.5
	Winter	6.5 ± 0.5	3.2 ± 0.1	-28.2 ± 0.2	23.0 ± 6.3
Kolyma	Spring	6.4 ± 1.6	2.8 ± 0.3	-28.9 ± 0.4	12.1 ± 25.4
	Summer	4.5 ± 0.3	2.6 ± 0.1	-29.2 ± 0.2	-30.5 ± 9.6
	Winter	3.5 ± 0.2	1.9 ± 0.1	-28.7 ± 0.3	-58.5 ± 7.8
Yukon	Spring	5.3 ± 0.9	2.9 ± 0.3	-29.6 ± 0.4	-58.9 ± 42.8
	Summer	5.3 ± 0.5	3.0 ± 0.1	-28.4 ± 0.6	-82.0 ± 16.0
	Winter	3.2 ± 0.4	2.4 ± 0.1	-26.8 ± 0.9	-150.0 ± 13.5

Mackenzie	Spring	6.5 ± 0.4	2.8 ± 0.2	-29.0 ± 1.2	9.7 ± 12.7
	Summer	4.1 ± 0.3	2.5 ± 0.1	-26.3 ± 0.8	-37.3 ± 9.9
	Winter	4.0 ± 0.2	2.1 ± 0.1	-25.9 ± 0.7	-16.9 ± 5.6

Table 2. FT-ICR MS compound class and island of stability (IOS) and core Arctic riverine fingerprint (CARF) percent relative abundances across the six great Arctic Rivers from June 2012 to December 2017 (or January 2018 for the Yukon) (mean ± standard error) during spring (May and June), summer (July-October), and winter (November-April).

River	Season	n	Condensed Aromatics (%RA)	Polyphenolics (%RA)	HUPs (%RA)	Aliphatics (%RA)	Sugar-like (%RA)	Peptide-like (%RA)	IOS (%RA)	CARF (%RA)
Ob'	Spring	6	3.6 ± 0.4	11.5 ± 0.8	77.6 ± 1.5	6.1 ± 0.5	0.9 ± 0.1	0.4 ± 0.2	24.9 ± 1.6	67.2 ± 3.2
	Summer	12	3.0 ± 0.2	11.2 ± 0.3	79.6 ± 0.6	5.1 ± 0.3	0.7 ± 0.1	0.3 ± 0.1	26.3 ± 0.7	66.3 ± 1.9
	Winter	16	1.9 ± 0.1	9.2 ± 0.3	82.7 ± 0.3	5.3 ± 0.2	0.5 ± 0.1	0.4 ± 0.0	28.8 ± 0.6	67.5 ± 1.2
Yenisey	Spring	6	2.8 ± 0.5	10.2 ± 1.2	81.0 ± 1.7	4.9 ± 0.2	0.8 ± 0.2	0.4 ± 0.1	26.0 ± 1.6	65.2 ± 1.7
	Summer	12	2.3 ± 0.1	9.2 ± 0.3	82.6 ± 0.4	5.0 ± 0.3	0.7 ± 0.1	0.3 ± 0.1	28.2 ± 0.6	66.8 ± 1.2
	Winter	16	1.9± 0.2	8.0 ± 0.4	84.3 ± 0.8	5.1 ± 0.1	0.4 ± 0.1	0.4 ± 0.1	29.4 ± 0.8	66.7 ± 1.5
Lena	Spring	6	3.4 ± 0.4	11.0 ± 0.6	79.3 ± 1.3	5.2 ± 0.6	0.8 ± 0.1	0.4 ± 0.2	23.4 ± 1.2	62.1 ± 2.4
	Summer	11	2.3 ± 0.1	8.7 ± 0.2	83.1 ± 0.5	4.8 ± 0.3	0.7 ± 0.1	0.4 ± 0.1	28.4 ± 0.6	67.7 ± 1.1
	Winter	16	2.4 ± 0.1	9.0 ± 0.3	83.0 ± 0.5	5.0 ± 0.2	0.5 ± 0.1	0.3 ± 0.1	27.4 ± 0.8	66.2 ± 1.8
Kolyma	Spring	6	2.5 ± 0.7	8.3 ± 1.3	81.6 ± 2.8	6.2 ± 0.8	0.8 ± 0.2	0.7 ± 0.2	26.0 ± 1.7	65.1 ± 1.6
	Summer	12	1.4 ± 0.1	6.8 ± 0.2	86.1 ± 0.4	4.9 ± 0.2	0.5 ± 0.0	0.4 ± 0.1	28.9 ± 0.8	66.0 ± 1.4

	Winter	14	0.7 ± 0.1	4.7 ± 0.2	88.2 ± 0.3	5.4 ± 0.2	0.4 ± 0.0	0.7 ± 0.1	32.2 ± 0.8	69.3 ± 1.4
Yukon	Spring	4	2.4 ± 0.5	9.1 ± 0.9	81.4 ± 1.5	5.9 ± 0.5	0.6 ± 0.1	0.6 ± 0.1	26.3 ± 0.7	66.4 ± 1.0
	Summer	10	2.4 ± 0.1	9.7 ± 0.3	82.3 ± 0.4	4.6 ± 0.2	0.6 ± 0.1	0.3 ± 0.1	27.7 ± 0.5	67.9 ± 1.1
	Winter	14	1.6 ± 0.2	7.5 ± 0.5	85.2 ± 0.6	5.0 ± 0.2	0.3 ± 0.1	0.5 ± 0.1	31.5 ± 0.8	71.5 ± 1.2
Mackenzie	Spring	5	2.2 ± 0.2	8.8 ± 0.2	83.3 ± 0.6	4.8 ± 0.4	0.6 ± 0.1	0.4 ± 0.1	26.3 ± 0.9	65.2 ± 2.0
	Summer	10	1.5 ± 0.1	7.2 ± 0.3	85.7 ± 0.5	5.0 ± 0.2	0.4 ± 0.0	0.3 ± 0.1	29.9 ± 0.7	69.4 ± 1.9
	Winter	18	1.2 ± 0.1	6.2 ± 0.1	86.1 ± 0.1	5.7 ± 0.2	0.5 ± 0.0	0.4 ± 0.1	30.6 ± 0.3	71.1 ± 0.6

References

Ahmed, R., Prowse, T., Dibike, Y., Bonsal, B., & O'Neil, H. (2020). Recent trends in freshwater influx to the Arctic Ocean from four major Arctic-draining rivers. *Water, 12*(4), 1189. https://doi.org/10.3390/w12041189

Ala-Aho, P., Soulsby, C., Pokrovsky, O., Kirpotin, S., Karlsson, J., Serikova, S., Manasypov, R., Lim, A., Krickov, I., & Kolesnichenko, L. (2018). Permafrost and lakes control river isotope composition across a boreal Arctic transect in the Western Siberian lowlands. *Environmental Research Letters, 13*(3), 034028. https://doi.org/10.1088/1748-9326/aaa4fe

Amon, R. M., & Meon, B. (2004). The biogeochemistry of dissolved organic matter and nutrients in two large Arctic estuaries and potential implications for our understanding of the Arctic Ocean system. *Marine Chemistry, 92*(1-4), 311-330. https://doi.org/10.1016/j.marchem.2004.06.034

Amon, R. M., Rinehart, A., Duan, S., Louchouarn, P., Prokushkin, A., Guggenberger, G., Bauch, D., Stedmon, C., Raymond, P., & Holmes, R. (2012). Dissolved organic matter sources in large Arctic rivers. *Geochimica et Cosmochimica Acta, 94*, 217-237.

Antony, R., Willoughby, A. S., Grannas, A. M., Catanzano, V., Sleighter, R. L., Thamban, M., Hatcher, P. G., & Nair, S. (2017). Molecular insights on dissolved organic matter transformation by supraglacial microbial communities. *Environmental science & technology, 51*(8), 4328-4337. https://doi.org/10.1021/acs.est.6b05780

Arnell, N. W. (2005). Implications of climate change for freshwater inflows to the Arctic Ocean. *Journal of Geophysical Research: Atmospheres, 110*(D07105). https://doi.org/10.1029/2004JD005348

Arrieta, J. M., Mayol, E., Hansman, R. L., Herndl, G. J., Dittmar, T., & Duarte, C. M. (2015). Dilution limits dissolved organic carbon utilization in the deep ocean. *science, 348*(6232), 331-333.

Barrett, T., Robinson, E., Usenko, S., & Sheesley, R. (2015). Source contributions to wintertime elemental and organic carbon in the western Arctic based on radiocarbon and tracer apportionment. *Environmental science & technology, 49*(19), 11631-11639. https://doi.org/10.1021/acs.est.5b03081

Bayer, B., Hansman, R. L., Bittner, M. J., Noriega-Ortega, B. E., Niggemann, J., Dittmar, T., & Herndl, G. J. (2019). Ammonia-oxidizing archaea release a suite of organic compounds potentially fueling prokaryotic heterotrophy in the ocean. *Environ Microbiol, 21*(11), 4062-4075. https://doi.org/10.1111/1462-2920.14755

Behnke, M. I., Stubbins, A., Fellman, J. B., Hood, E., Dittmar, T., & Spencer, R. G. M. (2020). Dissolved organic matter sources in glacierized watersheds delineated through compositional and carbon isotopic modeling. *Limnology and Oceanography*. https://doi.org/10.1002/lno.11615

Bell, L. E., Bluhm, B. A., & Iken, K. (2016). Influence of terrestrial organic matter in marine food webs of the Beaufort Sea shelf and slope. *Marine Ecology Progress Series, 550*, 1-24. https://doi.org/10.3354/meps11725

Blaen, P. J., Hannah, D. M., Brown, L. E., & Milner, A. M. (2014). Water source dynamics of high Arctic river basins. *Hydrological Processes, 28*(10), 3521-3538. https://doi.org/10.1002/hyp.9891

Bolduc, C., Lamoureux, S. F., & Franssen, J. (2018). Thermal and isotopic evidence for surface and subsurface water contributions to baseflow in a high Arctic river. *Hydrological Processes, 32*(5), 602-616. https://doi.org/10.1002/hyp.11427

Boucher, J. L., & Carey, S. K. (2010). Exploring runoff processes using chemical, isotopic and hydrometric data in a discontinuous permafrost catchment. *Hydrology Research, 41*(6), 508-519. https://doi.org/10.2166/nh.2010.146

Bring, A., Fedorova, I., Dibike, Y., Hinzman, L., Mård, J., Mernild, S., Prowse, T., Semenova, O., Stuefer, S. L., & Woo, M. K. (2016). Arctic terrestrial hydrology: A synthesis of processes, regional effects, and research challenges. *Journal of Geophysical Research: Biogeosciences, 121*(3), 621-649. https://doi.org/10.1002/2015JG003131

Carmack, E. C., Yamamoto-Kawai, M., Haine, T. W., Bacon, S., Bluhm, B. A., Lique, C., Melling, H., Polyakov, I. V., Straneo, F., & Timmermans, M. L. (2016). Freshwater and its role in the Arctic Marine System: Sources, disposition, storage, export, and physical and biogeochemical consequences in the Arctic and global oceans. *Journal of Geophysical Research: Biogeosciences, 121*(3), 675-717. https://doi.org/10.1002/2015JG003140

Casper, A. F., Rautio, M., Martineau, C., & Vincent, W. (2015). Variation and assimilation of Arctic riverine sestonin the pelagic food web of the Mackenzie

River Delta and Beaufort Sea Transition Zone. *Estuaries and Coasts, 38*(5), 1656-1663. https://doi.org/10.1007/s12237-014-9917-z

Chapelle, F. H., Shen, Y., Strom, E. W., & Benner, R. (2016). The removal kinetics of dissolved organic matter and the optical clarity of groundwater. *Hydrogeology Journal, 24*(6), 1413-1422. https://doi.org/10.1007/s10040-016-1406-y

Clark, I. D., Lauriol, B., Harwood, L., & Marschner, M. (2001). Groundwater contributions to discharge in a permafrost setting, Big Fish River, NWT, Canada. *Arctic, Antarctic, and Alpine Research, 33*(1), 62-69. https://doi.org/10.1080/15230430.2001.12003405

Connolly, C. T., Cardenas, M. B., Burkart, G. A., Spencer, R. G., & McClelland, J. W. (2020). Groundwater as a major source of dissolved organic matter to Arctic coastal waters. *Nature communications, 11*(1), 1-8. https://doi.org/10.1038/s41467-020-15250-8

Corilo, Y. (2015). PetroOrg: Florida State University.

D'Andrilli, J., Cooper, W. T., Foreman, C. M., & Marshall, A. G. (2015). An ultrahigh-resolution mass spectrometry index to estimate natural organic matter lability. *Rapid communications in mass spectrometry, 29*(24), 2385-2401. https://doi.org/10.1002/rcm.7400

Dittmar, T., Koch, B., Hertkorn, N., & Kattner, G. (2008). A simple and efficient method for the solid-phase extraction of dissolved organic matter (SPE-DOM) from seawater. *Limnology and Oceanography: Methods, 6*(6), 230-235. https://doi.org/10.4319/lom.2008.6.230

Douglas, T. A., Blum, J. D., Guo, L., Keller, K., & Gleason, J. D. (2013). Hydrogeochemistry of seasonal flow regimes in the Chena River, a subarctic watershed draining discontinuous permafrost in interior Alaska (USA). *Chemical Geology, 335*, 48-62. https://doi.org/10.1016/j.chemgeo.2012.10.045

Drake, T. W., Guillemette, F., Hemingway, J. D., Chanton, J. P., Podgorski, D. C., Zimov, N. S., & Spencer, R. G. (2018). The ephemeral signature of permafrost carbon in an Arctic fluvial network. *Journal of Geophysical Research: Biogeosciences, 123*(5), 1475-1485. https://doi.org/10.1029/2017JG004311

Drake, T. W., Tank, S. E., Zhulidov, A. V., Holmes, R. M., Gurtovaya, T., & Spencer, R. G. (2018). Increasing alkalinity export from large Russian Arctic rivers. *Environmental science & technology, 52*(15), 8302-8308.

Dunton, K. H., Schonberg, S. V., & Cooper, L. W. (2012). Food web structure of the Alaskan nearshore shelf and estuarine lagoons of the Beaufort Sea. *Estuaries and Coasts, 35*(2), 416-435. https://doi.org/10.1007/s12237-012-9475-1

Dunton, K. H., Weingartner, T., & Carmack, E. C. (2006). The nearshore western Beaufort Sea ecosystem: circulation and importance of terrestrial carbon in arctic coastal food webs. *Progress in Oceanography, 71*(2-4), 362-378. https://doi.org/10.1016/j.pocean.2006.09.011

Durocher, M., Requena, A. I., Burn, D. H., & Pellerin, J. (2019). Analysis of trends in annual streamflow to the Arctic Ocean. *Hydrological Processes, 33*(7), 1143-1151. https://doi.org/10.1002/hyp.13392

Fellman, J. B., D'Amore, D. V., Hood, E., & Boone, R. D. (2008). Fluorescence characteristics and biodegradability of dissolved organic matter in forest and wetland soils from coastal temperate watersheds in southeast Alaska. *Biogeochemistry, 88*(2), 169-184. https://doi.org/10.1007/s10533-008-9203-x

Fellman, J. B., Hood, E., Spencer, R. G., Stubbins, A., & Raymond, P. A. (2014). Watershed glacier coverage influences dissolved organic matter biogeochemistry in coastal watersheds of Southeast Alaska. *Ecosystems, 17*(6), 1014-1025. https://doi.org/10.1007/s10021-014-9777-1

Feng, L., Xu, J., Kang, S., Li, X., Li, Y., Jiang, B., & Shi, Q. (2016). Chemical composition of microbe-derived dissolved organic matter in cryoconite in Tibetan Plateau glaciers: insights from Fourier transform ion cyclotron resonance mass spectrometry analysis. *Environmental science & technology, 50*(24), 13215-13223. https://doi.org/10.1021/acs.est.6b03971

Fouché, J., Lafrenière, M. J., Rutherford, K., & Lamoureux, S. (2017). Seasonal hydrology and permafrost disturbance impacts on dissolved organic matter composition in High Arctic headwater catchments. *Arctic Science, 3*(2), 378-405. https://doi.org/10.1139/as-2016-0031

Fox, J., & Weisberg, S. (2019). An Companion to Applied Regression, Third Edition. Thousand Oaks CA: Sage. Retrieved from https://socialsciences.mcmaster.ca/jfox/Books/Companion/

Frey, K. E., Siegel, D. I., & Smith, L. C. (2007). Geochemistry of west Siberian streams and their potential response to permafrost degradation. *Water Resources Research, 43*(3).

Furrer, R., Nychka, D., Sain, S., & Nychka, M. D. (2017). Fields: tools for spatial data. R package version 9.8-6.

Gandois, L., Hoyt, A. M., Hatté, C., Jeanneau, L., Teisserenc, R., Liotaud, M., & Tananaev, N. (2019). Contribution of peatland permafrost to dissolved organic matter along a thaw gradient in North Siberia. *Environmental science & technology, 53*(24), 14165-14174. https://doi.org/10.1021/acs.est.9b03735

Glotov, V., Glotova, L., & Ushakov, M. (2015). Groundwater resources in the Kolyma River valley and their changes caused by the operation of the Kolyma hydropower plant. *Water Resources, 42*(7), 869-875.

Guéguen, C., Guo, L., & Tanaka, N. (2005). Distributions and characteristics of colored dissolved organic matter in the western Arctic Ocean. *Continental Shelf Research, 25*(10), 1195-1207. https://doi.org/10.1016/j.csr.2005.01.005

Harrell, F. E. J., & Dupont, C. (2019). Hmisc: Harrell miscellaneous. R package version 4.2-0. *Online publication*.

Hendrickson, C. L., Quinn, J. P., Kaiser, N. K., Smith, D. F., Blakney, G. T., Chen, T., Marshall, A. G., Weisbrod, C. R., & Beu, S. C. (2015). 21 Tesla Fourier transform ion cyclotron resonance mass spectrometer: a national resource for ultrahigh resolution mass analysis. *Journal of the American Society for*

Mass Spectrometry, 26(9), 1626-1632. https://doi.org/10.1007/s13361-015-1182-2

Hernes, P. J., & Benner, R. (2006). Terrigenous organic matter sources and reactivity in the North Atlantic Ocean and a comparison to the Arctic and Pacific oceans. *Marine Chemistry, 100*(1-2), 66-79. https://doi.org/10.1016/j.marchem.2005.11.003

Hertkorn, N., Benner, R., Frommberger, M., Schmitt-Kopplin, P., Witt, M., Kaiser, K., Kettrup, A., & Hedges, J. I. (2006). Characterization of a major refractory component of marine dissolved organic matter. *Geochimica et Cosmochimica Acta, 70*(12), 2990-3010. https://doi.org/10.1016/j.gca.2006.03.021

Hiyama, T., Asai, K., Kolesnikov, A. B., Gagarin, L. A., & Shepelev, V. V. (2013). Estimation of the residence time of permafrost groundwater in the middle of the Lena River basin, eastern Siberia. *Environmental Research Letters, 8*(3), 035040.

Hodgkins, S. B., Tfaily, M. M., Podgorski, D. C., McCalley, C. K., Saleska, S. R., Crill, P. M., Rich, V. I., Chanton, J. P., & Cooper, W. T. (2016). Elemental composition and optical properties reveal changes in dissolved organic matter along a permafrost thaw chronosequence in a subarctic peatland. *Geochimica et Cosmochimica Acta, 187*, 123-140. https://doi.org/10.1016/j.gca.2016.05.015

Holmes, R. M., Coe, M. T., Fiske, G. J., Gurtovaya, T., McClelland, J. W., Shiklomanov, A. I., Spencer, R. G., Tank, S. E., & Zhulidov, A. V. (2013). Climate change impacts

on the hydrology and biogeochemistry of Arctic rivers *Climatic Change and Global Warming of Inland Waters* (pp. 1-26).

Holmes, R. M., McClelland, J. W., Peterson, B. J., Tank, S. E., Bulygina, E., Eglinton, T. I., Gordeev, V. V., Gurtovaya, T. Y., Raymond, P. A., & Repeta, D. J. (2012). Seasonal and annual fluxes of nutrients and organic matter from large rivers to the Arctic Ocean and surrounding seas. *Estuaries and Coasts, 35*(2), 369-382. https://doi.org/10.1007/s12237-011-9386-6

Holmes, R. M., McClelland, J. W., Raymond, P. A., Frazer, B. B., Peterson, B. J., & Stieglitz, M. (2008). Lability of DOC transported by Alaskan rivers to the Arctic Ocean. *Geophysical Research Letters, 35*(3). https://doi.org/10.1029/2007GL032837

Hood, E., Fellman, J., Spencer, R. G., Hernes, P. J., Edwards, R., D'amore, D., & Scott, D. (2009). Glaciers as a source of ancient and labile organic matter to the marine environment. *Nature, 462*(7276), 1044. https://doi.org/10.1038/nature08580

Hopkinson, C. S., Buffam, I., Hobbie, J., Vallino, J., Perdue, M., Eversmeyer, B., Prahl, F., Covert, J., Hodson, R., & Moran, M. A. (1998). Terrestrial inputs of organic matter to coastal ecosystems: an intercomparison of chemical characteristics and bioavailability. *Biogeochemistry, 43*(3), 211-234. https://doi.org/10.1023/A:1006016030299

Jiao, N., Herndl, G. J., Hansell, D. A., Benner, R., Kattner, G., Wilhelm, S. W., Kirchman, D. L., Weinbauer, M. G., Luo, T., & Chen, F. (2010). Microbial production of recalcitrant dissolved organic matter: long-term carbon storage in the global

ocean. *Nature Reviews Microbiology, 8*(8), 593. https://doi.org/10.1038/nrmicro2386

Johnston, S. E., Bogard, M. J., Rogers, J. A., Butman, D., Striegl, R. G., Dornblaser, M., & Spencer, R. G. (2019). Constraining dissolved organic matter sources and temporal variability in a model sub-Arctic lake. *Biogeochemistry, 146*(3), 271-292. https://doi.org/10.1007/s10533-019-00619-9(0123456789().,-volV() 0123458697().,-volV)

Johnston, S. E., Shorina, N., Bulygina, E., Vorobjeva, T., Chupakova, A., Klimov, S. I., Kellerman, A. M., Guillemette, F., Shiklomanov, A., Podgorski, D. C., & Spencer, R. (2018). Flux and seasonality of dissolved organic matter from the Northern Dvina (Severnaya Dvina) River, Russia. *Journal of Geophysical Research: Biogeosciences, 123*(3), 1041-1056. https://doi.org/10.1002/2017JG004337

Kaiser, K., Canedo-Oropeza, M., McMahon, R., & Amon, R. M. (2017). Origins and transformations of dissolved organic matter in large Arctic rivers. *Scientific Reports, 7*(1), 13064. https://doi.org/10.1038/s41598-017-12729-1

Kassambara, A. (2020). rstatix: Pipe-Friendly Framework for Basic Statistical Tests. . Retrieved from https://CRAN.R-project.org/package=rstatix

Kassambara, A., & Mundt, F. (2017). factoextra: extract and visualize the results of multivariate data analyses. R package version 1.0.5. Retrieved from https://CRAN.R-project.org/package=factoextra

Kellerman, A. M., Dittmar, T., Kothawala, D. N., & Tranvik, L. J. (2014). Chemodiversity of dissolved organic matter in lakes driven by climate and

hydrology. *Nature communications, 5*, 3804. https://doi.org/10.1038/ncomms4804

Kellerman, A. M., Guillemette, F. o., Podgorski, D. C., Aiken, G. R., Butler, K. D., & Spencer, R. G. (2018). Unifying concepts linking dissolved organic matter composition to persistence in aquatic ecosystems. *Environmental science & technology, 52*(5), 2538-2548. https://doi.org/10.1021/acs.est.7b05513

Kellerman, A. M., Kothawala, D. N., Dittmar, T., & Tranvik, L. J. (2015). Persistence of dissolved organic matter in lakes related to its molecular characteristics. *Nature Geoscience*. https://doi.org/10.1038/NGEO2440

Koch, B., & Dittmar, T. (2006). From mass to structure: an aromaticity index for high-resolution mass data of natural organic matter. *Rapid communications in mass spectrometry, 20*(5), 926-932. https://doi.org/10.1002/rcm.2386

Koch, B., & Dittmar, T. (2016). From mass to structure: an aromaticity index for high-resolution mass data of natural organic matter. *Rapid communications in mass spectrometry, 20*(5), 926-932. https://doi.org/10.1002/rcm.7433

Kujawinski, E. B., Del Vecchio, R., Blough, N. V., Klein, G. C., & Marshall, A. G. (2004). Probing molecular-level transformations of dissolved organic matter: insights on photochemical degradation and protozoan modification of DOM from electrospray ionization Fourier transform ion cyclotron resonance mass spectrometry. *Marine Chemistry, 92*(1-4), 23-37. https://doi.org/10.1016/j.marchem.2004.06.038

Lang, S. Q., McIntyre, C. P., Bernasconi, S. M., Früh-Green, G. L., Voss, B. M., Eglinton, T. I., & Wacker, L. (2016). Rapid 14 C analysis of dissolved organic carbon in

non-saline waters. *Radiocarbon, 58*(3), 505-515. https://doi.org/10.1017/RDC.2016.17

Lawson, E. C., Bhatia, M. P., Wadham, J. L., & Kujawinski, E. B. (2014). Continuous summer export of nitrogen-rich organic matter from the Greenland Ice Sheet inferred by ultrahigh resolution mass spectrometry. *Environmental science & technology, 48*(24), 14248-14257. https://doi.org/10.1021/es501732h

Lechtenfeld, O. J., Kattner, G., Flerus, R., McCallister, S. L., Schmitt-Kopplin, P., & Koch, B. P. (2014). Molecular transformation and degradation of refractory dissolved organic matter in the Atlantic and Southern Ocean. *Geochimica et Cosmochimica Acta, 126*, 321-337. https://doi.org/10.1016/j.gca.2013.11.009

Letscher, R. T., Hansell, D. A., & Kadko, D. (2011). Rapid removal of terrigenous dissolved organic carbon over the Eurasian shelves of the Arctic Ocean. *Marine Chemistry, 123*(1-4), 78-87. https://doi.org/10.1016/j.marchem.2010.10.002

Lique, C., Holland, M. M., Dibike, Y. B., Lawrence, D. M., & Screen, J. A. (2016). Modeling the Arctic freshwater system and its integration in the global system: Lessons learned and future challenges. *Journal of Geophysical Research: Biogeosciences, 121*(3), 540-566. https://doi.org/10.1002/2015JG003120

MacDonald, E. N., Tank, S. E., Kokelj, S. V., Froese, D. G., & Hutchins, R. H. (2021). Permafrost-derived dissolved organic matter composition varies across

permafrost end-members in the western Canadian Arctic. *Environmental Research Letters*, 16, 024036. https://doi.org/10.1088/1748-9326/abd971

Mann, P. J., Eglinton, T. I., McIntyre, C. P., Zimov, N., Davydova, A., Vonk, J. E., Holmes, R. M., & Spencer, R. G. (2015). Utilization of ancient permafrost carbon in headwaters of Arctic fluvial networks. *Nature communications, 6*, 7856. https://doi.org/10.1038/ncomms8856

Mann, P. J., Spencer, R. G., Hernes, P. J., Six, J., Aiken, G. R., Tank, S. E., McClelland, J. W., Butler, K. D., Dyda, R. Y., & Holmes, R. M. (2016). Pan-arctic trends in terrestrial dissolved organic matter from optical measurements. *Frontiers in Earth Science, 4*, 25. https://doi.org/10.3389/feart.2016.00025

Massicotte, P., Asmala, E., Stedmon, C., & Markager, S. (2017). Global distribution of dissolved organic matter along the aquatic continuum: Across rivers, lakes and oceans. *Science of the Total Environment, 609*, 180-191. https://doi.org/10.1016/j.scitotenv.2017.07.076

McClelland, J. W., Déry, S. J., Peterson, B. J., Holmes, R. M., & Wood, E. F. (2006). A pan-arctic evaluation of changes in river discharge during the latter half of the 20th century. *Geophysical Research Letters, 33*(6).

McClelland, J. W., Holmes, R., Dunton, K., & Macdonald, R. (2012). The Arctic ocean estuary. *Estuaries and Coasts, 35*(2), 353-368.

McClelland, J. W., Holmes, R. M., Peterson, B. J., Amon, R., Brabets, T., Cooper, L., Gibson, J., Gordeev, V. V., Guay, C., & Milburn, D. (2008). Development of a pan-Arctic database for river chemistry. *Eos, Transactions American*

Geophysical Union, 89(24), 217-218. https://doi.org/10.1029/2008EO240001

McClelland, J. W., Townsend-Small, A., Holmes, R., Pan, F., Stieglitz, M., Khosh, M., & Peterson, B. (2014). River export of nutrients and organic matter from the North Slope of Alaska to the Beaufort Sea. *Water Resources Research, 50*(2), 1823-1839.

McDonough, L. K., O'Carroll, D. M., Meredith, K., Andersen, M. S., Brugger, C., Huang, H., Rutlidge, H., Behnke, M. I., Spencer, R. G. M., McKenna, A., Marjo, C. E., Oudone, P., & Baker, A. (2020). Changes in groundwater dissolved organic matter character in a coastal sand aquifer due to rainfall recharge. *Water research, 169*, 115201. https://doi.org/10.1016/j.watres.2019.115201

McDonough, L. K., Rutlidge, H., O'Carroll, D. M., Andersen, M. S., Meredith, K., Behnke, M. I., Spencer, R. G., McKenna, A. M., Marjo, C. E., & Oudone, P. (2020). Characterisation of shallow groundwater dissolved organic matter in aeolian, alluvial and fractured rock aquifers. *Geochimica et Cosmochimica Acta*. https://doi.org/10.1016/j.gca.2020.01.022

McDonough, L. K., Santos, I. R., Andersen, M. S., O'Carroll, D. M., Rutlidge, H., Meredith, K., Oudone, P., Bridgeman, J., Gooddy, D. C., & Sorensen, J. P. (2020). Changes in global groundwater organic carbon driven by climate change and urbanization. *Nature communications, 11*(1), 1-10. https://doi.org/10.1038/s41467-020-14946-1

Musilova, M., Tranter, M., Wadham, J., Telling, J., Tedstone, A., & Anesio, A. M. (2017). Microbially driven export of labile organic carbon from the Greenland ice sheet. *Nature Geoscience, 10*(5), 360. https://doi.org/10.1038/ngeo2920

Nakata, K., Kodama, H., Hasegawa, T., Hama, K., Iwatsuki, T., & Miyajima, T. (2013). Groundwater dating using radiocarbon in fulvic acid in groundwater containing fluorescein. *Journal of hydrology, 489*, 189-200. https://doi.org/10.1016/j.jhydrol.2013.03.012

Neff, J., Finlay, J., Zimov, S., Davydov, S., Carrasco, J., Schuur, E., & Davydova, A. (2006). Seasonal changes in the age and structure of dissolved organic carbon in Siberian rivers and streams. *Geophysical Research Letters, 33*(23), L23401. https://doi.org/10.1029/2006GL028222

O'Donnell, J. A., Aiken, G. R., Butler, K. D., Guillemette, F., Podgorski, D. C., & Spencer, R. G. (2016). DOM composition and transformation in boreal forest soils: The effects of temperature and organic-horizon decomposition state. *Journal of Geophysical Research: Biogeosciences, 121*(10), 2727-2744. https://doi.org/10.1002/2016JG003431

O'Donnell, J. A., Aiken, G. R., Swanson, D. K., Panda, S., Butler, K. D., & Baltensperger, A. P. (2016). Dissolved organic matter composition of Arctic rivers: Linking permafrost and parent material to riverine carbon. *Global Biogeochemical Cycles*, *30*(12), 1811-1826. https://doi.org/ 10.1002/2016GB005482

O'Donnell, J. A., Aiken, G. R., Walvoord, M. A., & Butler, K. D. (2012). Dissolved organic matter composition of winter flow in the Yukon River basin:

Implications of permafrost thaw and increased groundwater discharge. *Global Biogeochemical Cycles, 26*(4).

O'Donnell, J. A., Carey, M. P., Koch, J. C., Xu, X., Poulin, B. A., Walker, J., & Zimmerman, C. E. (2019). Permafrost Hydrology Drives the Assimilation of Old Carbon by Stream Food Webs in the Arctic. *Ecosystems*, 1-19. https://doi.org/10.1007/s10021-019-00413-6

Oksanen, J., Blanchet, F. G., Kindt, R., Legendre, P., O'hara, R., Simpson, G. L., Solymos, P., Stevens, M. H. H., & Wagner, H. (2019). Vegan: community ecology package. R package version 2.5-6.

Pabich, W. J., Valiela, I., & Hemond, H. F. (2001). Relationship between DOC concentration and vadose zone thickness and depth below water table in groundwater of Cape Cod, USA. *Biogeochemistry, 55*(3), 247-268. https://doi.org/10.1023/A:1011842918260

Perminova, I., Shirshin, E., Zherebker, A., Pipko, I., Pugach, S., Dudarev, O., Nikolaev, E., Grigoryev, A., Shakhova, N., & Semiletov, I. (2019). Signatures of Molecular Unification and progressive oxidation Unfold in Dissolved organic Matter of the ob-irtysh River System along its path to the Arctic ocean. *Scientific Reports, 9*(1), 1-16.

Peterson, B. J., Holmes, R. M., McClelland, J. W., Vörösmarty, C. J., Lammers, R. B., Shiklomanov, A. I., Shiklomanov, I. A., & Rahmstorf, S. (2002). Increasing river discharge to the Arctic Ocean. *science, 298*(5601), 2171-2173. https://doi.org/10.1126/science.1077445

Pollard, W. H. (2005). Icing processes associated with high arctic perennial springs, Axel Heiberg Island, Nunavut, Canada. *Permafrost and Periglacial Processes, 16*(1), 51-68.

Prowse, T. D., Wrona, F. J., Reist, J. D., Gibson, J. J., Hobbie, J. E., Lévesque, L. M., & Vincent, W. F. (2006). Climate change effects on hydroecology of Arctic freshwater ecosystems. *AMBIO: A Journal of the Human Environment, 35*(7), 347-358. https://doi.org/10.1579/0044-7447(2006)35[347:CCEOHO]2.0.CO;2

R Core Team. (2019). R: A language and environment for statistical computing. Vienna, Austria: R Foundation for Statistical Computing. Retrieved from https://www.R-project.org/

Rawlins, M. A., Steele, M., Holland, M. M., Adam, J. C., Cherry, J. E., Francis, J. A., Groisman, P. Y., Hinzman, L. D., Huntington, T. G., & Kane, D. L. (2010). Analysis of the Arctic system for freshwater cycle intensification: Observations and expectations. *Journal of Climate, 23*(21), 5715-5737. https://doi.org/10.1175/2010JCLI3421.1

Raymond, P. A., & Bauer, J. E. (2001a). Use of 14C and 13C natural abundances for evaluating riverine, estuarine, and coastal DOC and POC sources and cycling: a review and synthesis. *Organic Geochemistry, 32*(4), 469-485. https://doi.org/10.1016/S0146-6380(00)00190-X

Raymond, P. A., & Bauer, J. E. (2001b). DOC cycling in a temperate estuary: a mass balance approach using natural 14C and 13C isotopes. *Limnology and Oceanography, 46*(3), 655-667.

Raymond, P. A., McClelland, J., Holmes, R., Zhulidov, A., Mull, K., Peterson, B., Striegl, R., Aiken, G., & Gurtovaya, T. (2007). Flux and age of dissolved organic carbon exported to the Arctic Ocean: A carbon isotopic study of the five largest arctic rivers. *Global Biogeochemical Cycles, 21*(4). https://doi.org/10.1029/2007GB002934

Raymond, P. A., Saiers, J. E., & Sobczak, W. V. (2016). Hydrological and biogeochemical controls on watershed dissolved organic matter transport: Pulse-shunt concept. *Ecology, 97*(1), 5-16. https://doi.org/10.1890/14-1684.1

Ruff, M., Fahrni, S., Gäggeler, H., Hajdas, I., Suter, M., Synal, H., Szidat, S., & Wacker, L. (2010). On-line radiocarbon measurements of small samples using elemental analyzer and MICADAS gas ion source. *Radiocarbon, 52*(4), 1645-1656.

Schiff, S., Aravena, R., Trumbore, S. E., Hinton, M., Elgood, R., & Dillon, P. (1997). Export of DOC from forested catchments on the Precambrian Shield of Central Ontario: clues from 13C and 14C. *Biogeochemistry, 36*(1), 43-65. https://doi.org/10.1023/A:1005744131385

Schuur, E., McGuire, A., Schädel, C., Grosse, G., Harden, J., Hayes, D., Hugelius, G., Koven, C., Kuhry, P., & Lawrence, D. (2015). Climate change and the permafrost carbon feedback. *Nature, 520*(7546), 171-179. https://doi.org/10.1038/nature14338

Schwab, M. S., Hilton, R. G., Raymond, P. A., Haghipour, N., Amos, E., Tank, S. E., Holmes, R. M., Tipper, E. T., & Eglinton, T. I. (2020). An abrupt aging of

dissolved organic carbon in large Arctic rivers. *Geophysical research letters*, *47*(23). https://doi.org/10.1029/2020GL088823

Seidel, M., Yager, P. L., Ward, N. D., Carpenter, E. J., Gomes, H. R., Krusche, A. V., Richey, J. E., Dittmar, T., & Medeiros, P. M. (2015). Molecular-level changes of dissolved organic matter along the Amazon River-to-ocean continuum. *Marine Chemistry, 177*, 218-231. https://doi.org/10.1016/j.marchem.2015.06.019

Serreze, M. C., & Barry, R. G. (2011). Processes and impacts of Arctic amplification: A research synthesis. *Global and Planetary Change, 77*(1-2), 85-96. https://doi.org/10.1016/j.gloplacha.2011.03.004

Sleighter, R. L., & Hatcher, P. G. (2008). Molecular characterization of dissolved organic matter (DOM) along a river to ocean transect of the lower Chesapeake Bay by ultrahigh resolution electrospray ionization Fourier transform ion cyclotron resonance mass spectrometry. *Marine Chemistry, 110*(3-4), 140-152. https://doi.org/10.1016/j.marchem.2008.04.008

Smith, D. F., Podgorski, D. C., Rodgers, R. P., Blakney, G. T., & Hendrickson, C. L. (2018). 21 tesla FT-ICR mass spectrometer for ultrahigh-resolution analysis of complex organic mixtures. *Analytical chemistry, 90*(3), 2041-2047. https://doi.org/10.1021/acs.analchem.7b04159

Smith, H. J., Foster, R. A., McKnight, D. M., Lisle, J. T., Littmann, S., Kuypers, M. M., & Foreman, C. M. (2017). Microbial formation of labile organic carbon in Antarctic glacial environments. *Nature Geoscience, 10*(5), 356. https://doi.org/10.1093/femsec/fiy090

Smith, H. J., Tigges, M., D'Andrilli, J., Parker, A., Bothner, B., & Foreman, C. (2018). Dynamic processing of DOM: Insight from exometabolomics, fluorescence spectroscopy, and mass spectrometry. *Limnology and Oceanography Letters, 3*(3), 225-235. https://doi.org/10.1002/lol2.10082

Smith, L. C., Pavelsky, T. M., MacDonald, G. M., Shiklomanov, A. I., & Lammers, R. B. (2007). Rising minimum daily flows in northern Eurasian rivers: A growing influence of groundwater in the high-latitude hydrologic cycle. *Journal of Geophysical Research: Biogeosciences, 112*(G4). https://doi.org/10.1029/2006JG000327

Song, C., Wang, G., Mao, T., Dai, J., & Yang, D. (2020). Linkage between permafrost distribution and river runoff changes across the Arctic and the Tibetan Plateau. *Science China Earth Sciences, 63*(2), 292-302. https://doi.org/10.1007/s11430-018-9383-6

Spencer, R. G., Ahad, J. M., Baker, A., Cowie, G. L., Ganeshram, R., Upstill-Goddard, R. C., & Uher, G. (2007). The estuarine mixing behaviour of peatland derived dissolved organic carbon and its relationship to chromophoric dissolved organic matter in two North Sea estuaries (UK). *Estuarine, Coastal and Shelf Science, 74*(1-2), 131-144.

Spencer, R. G., Guo, W., Raymond, P. A., Dittmar, T., Hood, E., Fellman, J., & Stubbins, A. (2014). Source and biolability of ancient dissolved organic matter in glacier and lake ecosystems on the Tibetan Plateau. *Geochimica et Cosmochimica Acta, 142*, 64-74. https://doi.org/10.1016/j.gca.2014.08.006

Spencer, R. G., Kellerman, A. M., Podgorski, D. C., Macedo, M. N., Jankowski, K., Nunes, D., & Neill, C. (2019). Identifying the molecular signatures of agricultural expansion in Amazonian headwater streams. *Journal of Geophysical Research: Biogeosciences, 124*(6), 1637-1650. https://doi.org/10.1029/2018JG004910

Spencer, R. G., Mann, P. J., Dittmar, T., Eglinton, T. I., McIntyre, C., Holmes, R. M., Zimov, N., & Stubbins, A. (2015). Detecting the signature of permafrost thaw in Arctic rivers. *Geophysical Research Letters, 42*(8), 2830-2835. https://doi.org/10.1002/2015GL063498

Striegl, R. G., Dornblaser, M. M., Aiken, G. R., Wickland, K. P., & Raymond, P. A. (2007). Carbon export and cycling by the Yukon, Tanana, and Porcupine rivers, Alaska, 2001–2005. *Water Resources Research, 43*(2).

Stubbins, A., & Dittmar, T. (2015). Illuminating the deep: Molecular signatures of photochemical alteration of dissolved organic matter from North Atlantic Deep Water. *Marine Chemistry, 177*, 318-324. https://doi.org/10.1016/j.marchem.2015.06.020

Stubbins, A., Mann, P. J., Powers, L., Bittar, T. B., Dittmar, T., McIntyre, C. P., Eglinton, T. I., Zimov, N., & Spencer, R. G. (2017). Low photolability of yedoma permafrost dissolved organic carbon. *Journal of Geophysical Research: Biogeosciences, 122*(1), 200-211. https://doi.org/10.1002/2016JG003688

Stubbins, A., Spencer, R. G., Chen, H., Hatcher, P. G., Mopper, K., Hernes, P. J., Mwamba, V. L., Mangangu, A. M., Wabakanghanzi, J. N., & Six, J. (2010). Illuminated darkness: molecular signatures of Congo River dissolved organic matter and its photochemical alteration as revealed by ultrahigh precision

mass spectrometry. *Limnology and Oceanography, 55*(4), 1467-1477. https://doi.org/10.4319/lo.2010.55.4.1467

Tank, S. E., Fellman, J. B., Hood, E., & Kritzberg, E. S. (2018). Beyond respiration: Controls on lateral carbon fluxes across the terrestrial-aquatic interface. *Limnology and Oceanography Letters, 3*(3), 76-88. https://doi.org/10.1002/lol2.10065

Tank, S. E., Raymond, P. A., Striegl, R. G., McClelland, J. W., Holmes, R. M., Fiske, G. J., & Peterson, B. J. (2012). A land-to-ocean perspective on the magnitude, source and implication of DIC flux from major Arctic rivers to the Arctic Ocean. *Global Biogeochemical Cycles, 26*(4).

Tetzlaff, D., Buttle, J., Carey, S. K., McGuire, K., Laudon, H., & Soulsby, C. (2015). Tracer-based assessment of flow paths, storage and runoff generation in northern catchments: A review. *Hydrological Processes, 29*(16), 3475-3490. https://doi.org/10.1002/hyp.10412

Textor, S., Wickland, K., Podgorski, D., Johnston, S. E., & Spencer, R. G. M. (2019). Dissolved organic carbon turnover in permafrost-influenced watersheds of interior Alaska: Molecular insights and the priming effect. *Frontiers in Earth Science, 7*, 275. https://doi.org/10.3389/feart.2019.00275

Tipping, E., Billett, M., Bryant, C., Buckingham, S., & Thacker, S. (2010). Sources and ages of dissolved organic matter in peatland streams: evidence from chemistry mixture modelling and radiocarbon data. *Biogeochemistry, 100*(1-3), 121-137. https://doi.org/10.1007/s10533-010-9409-6

Tremblay, J.-É., Anderson, L. G., Matrai, P., Coupel, P., Bélanger, S., Michel, C., & Reigstad, M. (2015). Global and regional drivers of nutrient supply, primary production and CO2 drawdown in the changing Arctic Ocean. *Progress in Oceanography, 139*, 171-196. https://doi.org/10.1016/j.pocean.2015.08.009

Turetsky, M. R., Abbott, B. W., Jones, M. C., Anthony, K. W., Olefeldt, D., Schuur, E. A., Grosse, G., Kuhry, P., Hugelius, G., & McGuire, A. D. (2020). Carbon release through abrupt permafrost thaw. Nature Geoscience, 13(2), 138-143. https://doi.org/10.1038/s41561-019-0526-0

Vonk, J. E., Mann, P. J., Davydov, S., Davydova, A., Spencer, R. G., Schade, J., Sobczak, W. V., Zimov, N., Zimov, S., & Bulygina, E. (2013). High biolability of ancient permafrost carbon upon thaw. *Geophysical Research Letters*, *40*(11), 2689-2693. https://doi.org/10.1002/grl.50348

Walsh, J., Anisimov, O., Hagen, J., Jakobsson, T., Oerlemans, J., Prowse, T., Romanovsky, V., Savelieva, N., Serreze, M., & Shiklomanov, A. (2005). *Cryosphere and hydrology* Retrieved from Cambridge, United Kingdom.

Walvoord, M. A., & Kurylyk, B. L. (2016). Hydrologic impacts of thawing permafrost—A review. *Vadose Zone Journal, 15*(6). https://doi.org/10.2136/vzj2016.01.0010

Walvoord, M. A., & Striegl, R. G. (2007). Increased groundwater to stream discharge from permafrost thawing in the Yukon River basin: Potential impacts on lateral export of carbon and nitrogen. *Geophysical Research Letters, 34*(12).

Walvoord, M. A., Voss, C. I., & Wellman, T. P. (2012). Influence of permafrost distribution on groundwater flow in the context of climate-driven permafrost

thaw: Example from Yukon Flats Basin, Alaska, United States. *Water Resources Research, 48*(7). https://doi.org/10.1029/2011WR011595

Ward, C. P., & Cory, R. M. (2015). Chemical composition of dissolved organic matter draining permafrost soils. *Geochimica et Cosmochimica Acta, 167*, 63-79. https://doi.org/10.1016/j.gca.2015.07.001

Wassenaar, L., Aravena, R., Hendry, J., & Fritz, P. (1991). Radiocarbon in dissolved organic carbon, a possible groundwater dating method: case studies from western Canada. *Water Resources Research, 27*(8), 1975-1986. https://doi.org/10.1029/91WR00504

Weishaar, J. L., Aiken, G. R., Bergamaschi, B. A., Fram, M. S., Fujii, R., & Mopper, K. (2003). Evaluation of specific ultraviolet absorbance as an indicator of the chemical composition and reactivity of dissolved organic carbon. *Environmental science & technology, 37*(20), 4702-4708. https://doi.org/10.1021/es030360x

Wickham, H. (2007). Reshaping data with the reshape package. *Journal of Statistical Software, 21*(12), 1-20.

Wickland, K. P., Aiken, G. R., Butler, K., Dornblaser, M. M., Spencer, R., & Striegl, R. G. (2012). Biodegradability of dissolved organic carbon in the Yukon River and its tributaries: Seasonality and importance of inorganic nitrogen. *Global Biogeochemical Cycles, 26*(4), GB0E03. https://doi.org/10.1029/2012GB004342

Wild, B., Andersson, A., Bröder, L., Vonk, J., Hugelius, G., McClelland, J. W., Song, W., Raymond, P. A., & Gustafsson, Ö. (2019). Rivers across the Siberian Arctic

unearth the patterns of carbon release from thawing permafrost. *Proceedings of the National Academy of Sciences, 116*(21), 10280-10285. https://doi.org/10.1073/pnas.1811797116

Williams, J. W., & Jackson, S. T. (2007). Novel climates, no-analog communities, and ecological surprises. *Frontiers in Ecology and the Environment, 5*(9), 475-482. https://doi.org/10.1029/91WR00504

Woo, M.-K., Kane, D. L., Carey, S. K., & Yang, D. (2008). Progress in permafrost hydrology in the new millennium. *Permafrost and Periglacial Processes, 19*(2), 237-254. https://doi.org/10.1002/ppp.613

Woo, M.-K. (2012). *Permafrost hydrology*: Springer Science & Business Media.

Xu, M., Kang, S., Wang, X., Wu, H., Hu, D., & Yang, D. (2020). Climate and hydrological changes in the Ob River Basin during 1936–2017. *Hydrological Processes, 34*(8), 1821-1836.

Yoshikawa, K., Hinzman, L. D., & Kane, D. L. (2007). Spring and aufeis (icing) hydrology in Brooks Range, Alaska. *Journal of Geophysical Research: Biogeosciences, 112*(G4).

Zheng, Q., Chen, Q., Cai, R., He, C., Guo, W., Wang, Y., Shi, Q., Chen, C., & Jiao, N. (2019). Molecular characteristics of microbially mediated transformations of Synechococcus-derived dissolved organic matter as revealed by incubation experiments. *Environmental microbiology, 21*(7), 2533-2543. https://doi.org/10.1111/1462-2920.14646

Zolkos, S., Krabbenhoft, D. P., Suslova, A., Tank, S. E., McClelland, J. W., Spencer, R. G., Shiklomanov, A., Zhulidov, A. V., Gurtovaya, T., & Zimov, N. (2020). Mercury

Export from Arctic Great Rivers. *Environmental science & technology, 54*(7), 4140-4148.